Efficient Numeracy in Language Models through Single-token Number Encodings

Linus Kreitner [*1] **Paul Hager** [*1 2 †] **Jonathan Mengedoht** [3] **Georgios Kaissis** [1 4] **Daniel Rueckert** [1 5 6] **Martin J. Menten** [1 5 6]

Abstract

To drive progress in science and engineering, large language models (LLMs) must be able to process large amounts of numerical data and solve long calculations efficiently. This is currently only possible through the use of external tools or extensive reasoning chains, either weakening the numerical representations of LLMs or limiting the length of problems they can solve. We show that frontier LLMs require excessive amounts of reasoning tokens to solve even basic calculations, which is exacerbated by their tokenization strategies that split single numbers into multiple tokens. This motivates the need for efficient and effective single-token number encodings. We introduce a set of desiderata for such encodings and show that existing approaches fail to fulfill them. To address these shortcomings, we propose *BitTokens*[1] , a novel encoding strategy that represents any number as a single token using its IEEE 754 binary floating-point representation. Through extensive experiments we show that our BitTokens allow even small language models to learn algorithms that solve basic arithmetic operations nearly perfectly. This newly gained efficiency could expand the length and complexity of problems language models can solve.

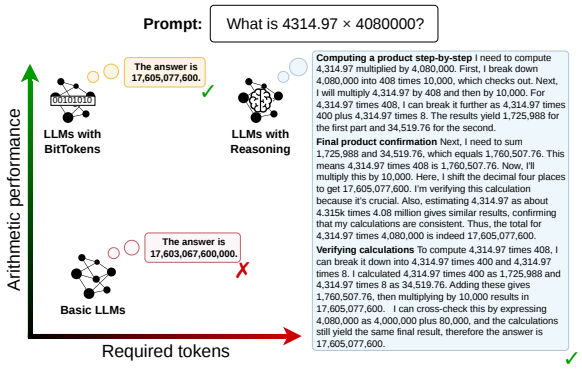

Figure 1. LLMs perform poorly on arithmetic tasks, requiring excessive reasoning tokens to achieve good performance. Our BitTokens tokenization strategy allows language models to solve arithmetic tasks both effectively and efficiently.

1. Introduction

Many researchers share the common vision that large language models (LLMs) will not only alleviate routine work but also drive scientific and technological innovation. In many fields, such as physics and engineering, solving such complex tasks requires the processing of large amounts of numerical data and extensive calculations. Thus, to aid advancements in these fields, LLMs must possess efficient and effective numeracy, defined as the ability to represent and compute numbers. However, LLMs have historically struggled to solve even basic calculations (AI4Science & Quantum, 2023; Cui et al., 2025; Hager et al., 2024). A growing body of work has thus tasked itself with finding the capabilities and limitations of transformers to perform mathematical operations (Charton, 2024; Lee et al., 2024; McLeish et al., 2024; Nogueira et al., 2021; Shen et al., 2023).

Research to improve the numeracy of LLMs has predominantly focused on two strategies: arithmetic tool use and reasoning chains. Tool-augmented LLMs leverage external calculators or code to bypass the need for internal arithmetic computation (Gao et al., 2023; Gou et al., 2024; Gu et al., 2024; He-Yueya et al., 2023; Le et al., 2022; Parisi

[*]Equal contribution [†] Work done while at TUM. [1]Chair for AI in Healthcare and Medicine, Technical University of Munich (TUM) and TUM University Hospital, Munich, Germany [2]Virtual Diagnostics Unit, QuantCo, Cambridge, MA, USA [3]TUM, Munich, Germany [4]Hasso Plattner Institute for Digital Engineering, University of Potsdam, Germany [5]Department of Computing, Imperial College London, UK [6]Munich Center for Machine Learning (MCML), Munich, Germany. Correspondence to: Linus Kreitner <linus.kreitner@tum.de>, Paul Hager <paul.hager@tum.de>.

Proceedings of the 43rd International Conference on Machine Learning, Seoul, South Korea. PMLR 306, 2026. Copyright 2026 by the author(s).

[1]Code available at https://github.com/KreitnerL/BitTokens

et al., 2022; Qu et al., 2025; Schick et al., 2023; Wang et al., 2024b; Zhang et al., 2023). While this approach guarantees the correctness of the calculations, it forces the model to dynamically and correctly identify, construct, and wait on all mathematical operations, introducing non-negligible latency and sources of error. Furthermore, outsourcing all calculations prevents the model from generating and calculating with intermediate numeric representations during a forward pass, restricting the efficiency of latent calculations(Hao et al., 2025; Lindsey et al., 2025; Skean et al., 2024).

Reasoning chains, on the other hand, prompt LLMs to generate logically consistent text, step-by-step, enabling them to solve complex problems by breaking them into smaller parts (Lightman et al., 2023; Snell et al., 2025; Wang et al., 2023; Wei et al., 2022; Yao et al., 2023). This has resulted in large gains on many benchmarks, pushing the frontier of what is possible with LLMs. However, reasoning chains can be very inefficient, sometimes requiring tens of thousands of tokens to solve a single calculation, as illustrated in Figure 1 and shown later. This limits the length and complexity of problems that LLMs can solve due to context window and cost constraints (Kwa et al., 2025).

We argue that both tooling and reasoning chains are merely crutches, allowing LLMs to solve arithmetic calculations but preventing them from obtaining the intrinsic numeric computation skills required to efficiently solve complex tasks in advanced technical domains. We hypothesize that addressing this problem requires rethinking the way LLMs tokenize and encode numbers. Existing tokenizers treat numbers the same as any other word, meaning they are parsed left to right and split based on a pre-defined vocabulary. This introduces an additional source of token inefficiency, especially in fields such as tabular language models that must ingest tens or hundreds of thousands of numbers (Akhtar et al., 2023; Hegselmann et al., 2023; Fang et al., 2024; Gardner et al., 2024; Liu et al., 2024; Zhang et al., 2025), and is not well suited for comparing and calculating numbers.

A series of works has tried to enhance this encoding step by adding information about the magnitude of numbers via additional tokens (Schwartz et al., 2024) or positional embeddings (McLeish et al., 2024). Others have aimed to address issues of left-to-right token prediction clashing with right-to-left carry-over logic by changing the order or formatting of digits during encoding (Baeumel et al., 2025; Lee et al., 2024; Singh & Strouse, 2024). While all these approaches improve upon standard encoding strategies, they still suffer from the efficiency concerns of single and triple digit tokenization strategies and fail to achieve perfect arithmetic performance.

The most ambitious line of works aims to completely change the way numbers are represented in LLMs, moving from representing individual digits or triplets of digits to encoding each number via a single specialized number token. Han et al. (2022) and Alberts et al. (2024) both employ small neural networks to generate such a number token based on the number's digits and its surrounding textual context. While this improves numeric computational ability, it suffers from similar efficiency drawbacks as conventional tokenization, requires auxiliary networks, and has only been tested for encoding. Ideally one would have a deterministic algorithm to encode numbers into and decode numbers from a fixed structure which would allow LLMs to learn calculation algorithms internally. Accordingly, Golkar et al. (2023) introduce xVal, which scales a learned number token by the numeric value. Zhou et al. (2026) propose FoNE, which encodes a number using sinusoidal functions of different frequencies. While conceptually interesting, we will demonstrate that both methods have fundamental shortcomings that render them ineffective number representations.

With the aim of evaluating and improving both the efficiency and numeracy of LLMs, this work makes the following three major contributions:

- We systematically evaluate the numeric computational ability of eight frontier LLMs across nine different tasks. We find that frontier LLMs strongly rely on reasoning chains with a large number of tokens to solve calculations (see Section 2).
- We develop a set of desiderata for efficient single-token number encodings that allows networks to learn algorithms that near perfectly execute numeric calculations (see Section 3). In an analysis of recent works, we show that existing single-token strategies fail to fulfill several key desiderata, limiting their potential to be used in LLMs (see Section 4).
- Guided by our desiderata, we propose BitTokens, a novel single-token encoding. Based on the IEEE 754 standard on binary floating-point numbers, BitTokens encode numbers as a sequence of bits representing the sign, exponent, and significand (see Section 5). We demonstrate our method's ability to generate structured, informative representations that allow even small language models to learn algorithms to solve basic arithmetic operations (see Section 6).

2. Evaluation of numeracy in frontier LLMs

Numeracy benchmarks for language models Mathematics is a core discipline on which LLMs are evaluated (Ahn et al., 2024; Chiang et al., 2024; Shao et al., 2024; Zhang et al., 2024). However, popular benchmarking datasets like GSM8K, MMLU-Pro, and Numeracy-600K are designed to test mathematical *reasoning* (Chen et al., 2019; Cobbe et al., 2021; Mirzadeh et al., 2025; Wang et al., 2024a). They

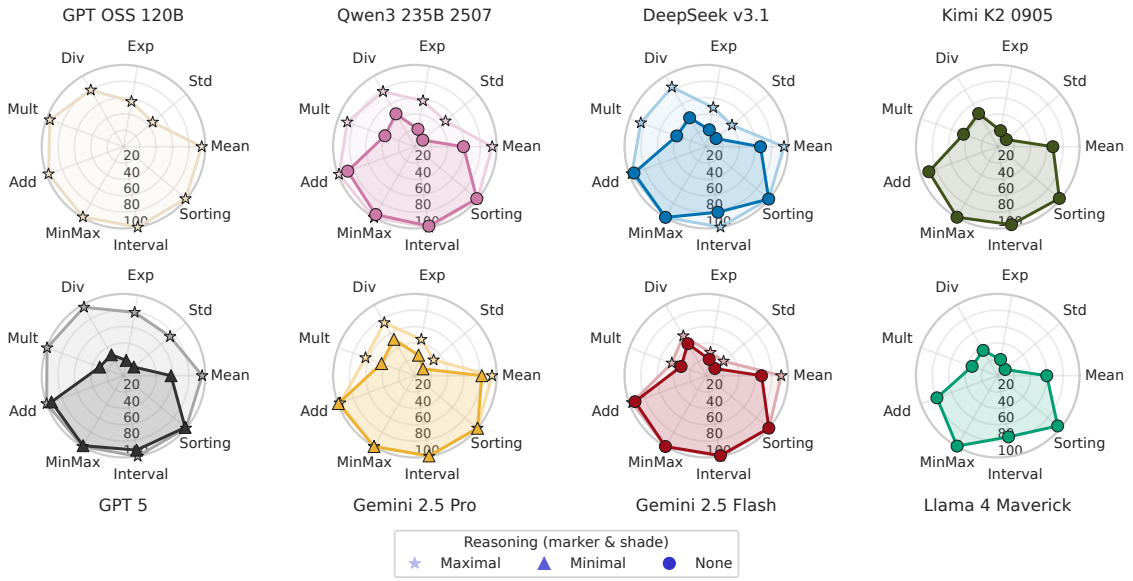

Figure 2. While simple tasks such as addition and sorting are almost perfectly solved by frontier LLMs, other tasks such as multiplication, division, calculating the standard deviation, or exponentiation remain difficult and require extensive reasoning tokens to solve.

primarily sample integers from narrow distributions and rely on text-based problems that conflate arithmetic with language understanding. Recently, a few benchmarks have attempted to isolate numeric computations. For example, NumericBench includes an arithmetic operations dataset, although it only tests integers with up to 6 digits and floats with up to 3 decimal places (Li et al., 2025). In contrast, The NumberCookbook tests a wide range of tasks and formats, including number comparisons and arithmetic on integers, floats, fractions, and scientific notation (Yang et al., 2025b). We create our own number dataset to add key operations such as division between floats, exponentiation, mean, and standard deviation. Additionally, we require full control over the operands' precision and the difficulty distribution of the arithmetic problems for proper training dynamics.

Tasks We design our tasks to isolate individual aspects of numeracy as well as core mathematical operations. The most basic task is to determine whether a numerical comparison of the form $n_1 \{<,>\} n_2$ holds true. To increase the difficulty of number comparisons, we test the ability to: (1) return the minimum or maximum of a list, (2) select the correct interval containing a number from a list of options, and (3) sort a list of numbers in ascending or descending order. To test the calculating capabilities of LLMs, we use all basic arithmetic operations including (4) addition / subtraction, (5) multiplication, and (6) division. Finally, we test the multi-step operations (7) exponentiation, (8) mean, and (9) standard deviation. See Appendix B.1 for examples.

Number sampling We utilize a custom number sampling strategy to ensure that we test a large diversity of inputs. Specifically, all generated numbers $n \in \mathbb{R}$ satisfy $n \in (-10^{15}, -10^{-14}] \cup [10^{-14}, 10^{15})$ and contain at most 15 significant decimal digits, defined as the total number of digits excluding leading and trailing zeros. Number magnitudes, differences between numbers, and precision are all densely and uniformly sampled. Further information can be found in Appendix B.2.

Evaluation metrics While exactly matching the true result is the correct answer, it is useful to know the relative error to compare models. To measure the relative error between a prediction $\hat{y}$ and the target y, the symmetric mean absolute percentage error (sMAPE) (Flores, 1986) is defined as:

$$\text{sMAPE}(\hat{y}, y) = \frac{|\hat{y} - y|}{|y| + |\hat{y}| + \varepsilon}, \quad \text{with } \epsilon = 10^{-100} \tag{1}$$

While this measures the relative error and is thus well suited for numbers and errors of different magnitudes, the metric decreases exponentially with increasing accuracy in significant figures. An error in the 4th significant digit can thus already achieve a sMAPE on the order of 10^{-4} despite the error being potentially very relevant in many real-world contexts. To address this, we propose the log-sMAPE score, which uses the base-10 logarithm of sMAPE divided by the total number of significant digits:

$$\text{log-sMAPE}(\hat{y}, y) = \min\left(1, \frac{\lg\left(\text{sMAPE}(\hat{y}, y) + \varepsilon\right)}{-M}\right) \tag{2}$$

Here $M = 15$ is the maximum number of significant digits tested. In essence, log-sMAPE calculates the fraction of significant figures correctly predicted until the first error. Thus, a log-sMAPE value of 0.2 indicates that the first 3

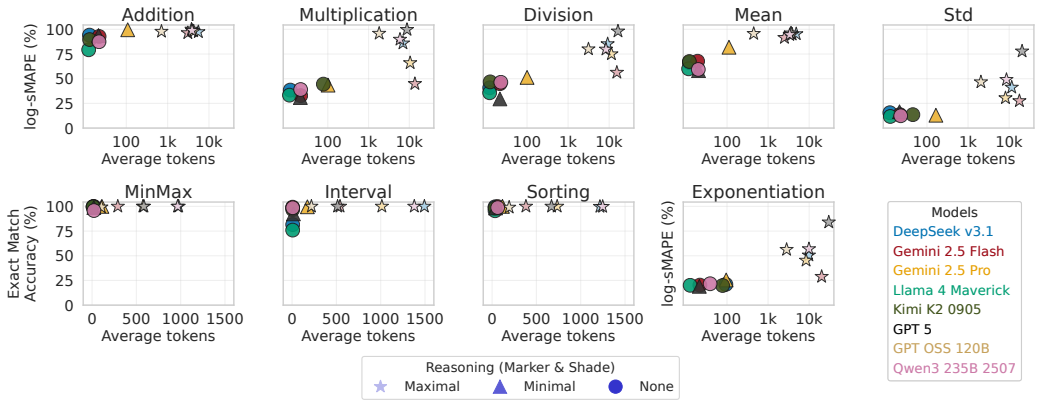

Figure 3. Difficult numeracy tasks such as multiplication, division, exponentiation, and standard deviation can only be solved by frontier models using excessive reasoning tokens.

out of 15 significant digits are correct. We use this metric in addition to exact match accuracy for the addition, multiplication, division, exponentiation, mean, and standard deviation tasks.

Results A radar plot of the results is shown in Figure 2 and an overview of the tested models and exact results can be found in Appendix C. It is important to note that we have no way of controlling what the proprietary models (such as GPT 5 and Gemini 2.5) do during the generation of their answer. While we very explicitly instruct them not to use calculators, see that their reasoning chains align with non-calculator use, and they often do not answer correctly, we have no guarantee that they do not use external tools. Their reported results should be seen as an upper bound.

Immediately apparent is the perfect accuracy of almost all models on the basic number comparison tasks of MinMax, Sorting, and Interval, which are effectively solved. When considering the basic arithmetic tasks, there is a clear separation between high reasoning and non- or minimal-reasoning models. While both perform excellently on addition and mean calculation, all non-reasoning models perform very poorly on multiplication, division, exponentiation, and standard deviation tasks, with none achieving above 60% log-sMAPE. Only once we allow a large number of reasoning tokens do we see improved performance on these tasks. This separation between thinking and non-thinking models is underscored in Figure 3. LLMs use between 5 and 30 thousand tokens to solve a single calculation. While future advances in post-training could reduce the number of reasoning tokens (Singhal et al., 2024; Yeo et al., 2025), it is clear that current LLMs rely heavily on reasoning chains to compensate for their poor native arithmetic performance. Such high token counts for just a single calculation make multi-step calculations and longer reasoning chains infeasible, thus motivating the need for a single-token number representation.

3. Desiderata for single-token number representation strategies

Our goal is to develop a number encoding strategy that generates representations which both maximize token efficiency and allow for neural networks to learn algorithms that perfectly execute numeric calculations. Such an algorithm or function must be injective and correct over the entire defined numeric input space. It also requires us to consider engineering realities, such as the normalization layers used, the numerical precision of the activation functions, and how gradient-based stochastic optimization learns representations:

D1 – Token efficiency: Every number is represented by a single token.

D2 – Uniqueness: Each value has exactly one valid encoding, with a unique inverse mapping.

D3 – Structured: The encoding geometry reflects numeric order and distance, facilitating generalizable algorithms.

D4 – Scale invariance: The desired range of input magnitudes and precisions can be represented.

D5 – Normalization: Encodings are bounded and information preserving under standard normalization functions used in language models (e.g., LayerNorm, RMSNorm).

D6 – Numerical stability: Representations remain accurate when using low-precision activations (e.g., FP8).

D7 – Continuity: Encodings vary smoothly with the underlying value, making them compatible with gradient-based optimization.

D8 – Robustness: Values can be decoded reliably under stochastic noise, allowing for stochastic training.

D9 – Arithmetic: Encodings admit learnable algorithms for core mathematical operations.

4. Establishing the limitations of existing single-token strategies using our desiderata

In this section we will analyze the two existing approaches – xVal (Golkar et al., 2023) and FoNE (Zhou et al., 2026) – for constructing single-token encodings and demonstrate why they are unsuitable using our desiderata. xVal introduces a trainable number token, [NUM], that is scaled by the numerical value being encoded. If a [NUM] token is predicted, the number can be decoded from the final hidden state through a separate number head. This approach satisfies D1 to D3 and D7. However, as shown by the authors, this strategy must map all inputs to the range [-5, 5] to satisfy D5 and avoid layer normalization interfering with the information encoded in the encoding magnitude. This causes it to be extremely limited in the range and precision of numbers it can encode, thus violating D4, D6, and by extension D9.

FoNE encodes a number in a single [NUM] token using Fourier features. Each dimension of the representation corresponds to either a sine or cosine function of base 10 with differing frequencies, each of which encodes the number before being added to a trainable [NUM] token. When a language model predicts a number token, the final hidden state can directly be interpreted as a sinusoidal encoding. The output number is predicted digit by digit through the maximum cosine similarity between each dimension of the final hidden state (corresponding to each digit of the output) with those of the encodings of the numbers in the range $[0, 9]$. This fulfills D1 to D8. In contrast to simply scaling a [NUM] token, using both sine and cosine functions equally guarantees a constant RMS norm, satisfying D5. Such a digit-wise maximum similarity decoding also allows for robustness to noise, satisfying D8.

The key limitation of sinusoidal encodings is that they are poorly suited for solving certain arithmetic operations with neural networks, most notably multiplication. In order to satisfy condition D9, we require a learnable mapping o' that computes the encoding, ξ, of the result of an operation o from the encodings of its operands:

$$\forall_o \, \exists_{o'} : \; \xi\big(o(x_1, \ldots, x_n)\big) \; = \; o'\big(\xi(x_1), \ldots, \xi(x_n)\big) \quad (3)$$

For addition, such a mapping exists and is computationally trivial.

Definition 4.1 (sinusoidal encoding). A sinusoidal encoding $\mathcal{F} : \mathbb{R} \mapsto \mathbb{T}^{|\Phi|}$ maps real numbers to a $|\Phi|$-dimensional torus, which forms a compact abelian Lie group. Given frequencies b^ϕ with base $b > 1$ and $\phi \in \Phi \subset \mathbb{Z}$, then $\mathcal{F}$ is defined as:

$$\mathcal{F}(x) := \left[\cos(2\pi b^\phi x), \, \sin(2\pi b^\phi x)\right]_{\phi \in \Phi} = \left[e^{i2\pi b^\phi x}\right]_{\phi \in \Phi} \quad (4)$$

Lemma 4.2 (additive homomorphism). *The encoding map $\mathcal{F}$ is a group homomorphism from the additive group of real numbers $(\mathbb{R}, +)$ to the multiplicative torus $(\mathbb{T}^{|\Phi|}, \odot)$, where $\odot$ denotes the element-wise (Hadamard) product.*

Proof. The claim follows directly from Euler's formula:

$$\begin{aligned} \mathcal{F}(x_1 + x_2) &= \left[e^{i2\pi b^\phi (x_1 + x_2)}\right]_{\phi \in \Phi} \\ &= \left[e^{i2\pi b^\phi x_1} e^{i2\pi b^\phi x_2}\right]_{\phi \in \Phi} = \mathcal{F}(x_1) \odot \mathcal{F}(x_2) \end{aligned} \quad (5)$$

Thus the encoding of the sum of two numbers x_1 and x_2 can be computed by a simple component-wise multiplication of their respective encodings. □

This homomorphism elegantly transforms addition in the number domain into a simple, local operation in the encoded domain. Notably, this operation does not require carry-over logic. However, for multiplication such a simple mapping does not exist.

Proposition 4.3 (complexity of multiplication). *Let $\mathcal{X} := \{\varepsilon, \ldots, U\}$ be the set of input numbers with resolution $\varepsilon = b^m$ and choose $\Phi = \{m, \ldots, n\}$ so that $\mathcal{F}$ uniquely encodes the entire number range. Assume each encoding component has a finite precision P (i.e., can represent P distinct states). Suppose there exists an operator $\otimes_\phi : \mathbb{T}^{|\Phi|} \times \mathbb{T}^{|\Phi|} \mapsto \mathbb{T}$ such that $\otimes_\phi(\mathcal{F}(x), \mathcal{F}(y)) := \mathcal{F}_\phi(xy)$ for each output frequency $\phi \in \Phi$. Let $S^x_\phi, S^y_\phi \subseteq \Phi$ be the subsets of input frequencies that $\otimes_\phi$ is required to take as input from $\mathcal{F}(x)$ and $\mathcal{F}(y)$, respectively. Then:*

1. ***Non-locality*** *The operator $\otimes_\phi$ must access at least $d = \mathcal{O}\left(\log_P(U/\varepsilon)\right)$ components from each input vector with $|S^x_\phi|, \; |S^y_\phi| \; \geq \; \lceil \log_P |\mathcal{X}| \rceil$.*

2. ***Computational complexity*** *The operator $\otimes$ must perform a computation functionally equivalent to polynomial multiplication.*

Proof. **1. Non-locality.** The proof follows from a counting argument. Assume for contradiction that $|S^x_\phi| < \log_P |\mathcal{X}|$. Then the projection of $\mathcal{F}(x)|_{S^x_\phi}$, which is the only information about x available to $\otimes_\phi$, can represent at most $P^{|S^x_\phi|}$ states. By the pigeonhole principle, there exist $x_1, x_2 \in \mathcal{X}$ with $x_1 \neq x_2$ that are indistinguishable to the operator, i.e., $\mathcal{F}(x_1)|_{S^x_\phi} = \mathcal{F}(x_2)|_{S^x_\phi}$. Let $\Delta := x_1 - x_2 \neq 0$. The set $Y^* := \{y \in \mathcal{X} : \; b^\phi \Delta y \in \mathbb{Z}\}$ is a proper subset of $\mathcal{X}$, so we can pick $y^\star \in \mathcal{X} \setminus Y^*$. Then $\mathcal{F}_\phi(x_1 y^\star) \neq \mathcal{F}_\phi(x_2 y^\star)$, yet $\otimes_\phi$ sees identical inputs from $\mathcal{F}(x_1)$ and $\mathcal{F}(x_2)$, which is a contradiction. The operator $\otimes_\phi$ is required by its definition to produce these two different outputs. However, since its inputs for x_1 and x_2 are identical ($\mathcal{F}(x_1)|_{S^x_\phi} = \mathcal{F}(x_2)|_{S^x_\phi}$), it is forced as a function to produce the same output for both. It cannot satisfy both conditions. Thus, the initial

assumption must be false and $|S^x_\phi| \geq \lceil \log_P |\mathcal{X}| \rceil$. The same holds for $|S^y_\phi|$.

2. Computational complexity. Multiplication in any positional system is equivalent to the discrete convolution of the coefficients k and l, followed by carry propagation.

Write $x = \sum_i k_i b^i$ and $y = \sum_j l_j b^j$ as the sum of their coefficients. Then

$$xy = \sum_\tau (k * l)_\tau b^\tau, \quad (k * l)_\tau = \sum_{i+j=\tau} k_i l_j. \tag{6}$$

Interpreting the circular sinusoidal component in its interval $[0, 1)$ wrap-around form, we can view the phase vector of the encoding, $\Theta_x \in [0, 1)^{|\Phi|}$, as a linear transformation of the coefficient vector k modulo 1. From the definition of the encoding, the component at frequency ϕ accumulates contributions from lower-order coefficients:

$$[\Theta_x]_\phi = \big(\sum_{i<\phi} k_i b^{i-\phi}\big) \bmod 1 \tag{7}$$

This forms a linear system $\Theta_x \equiv Mk \bmod 1$, where M is a lower-triangular mixing matrix with entries $M_{\phi,i} = b^{i-\phi}$ for $i < \phi$ and 0 otherwise. Since the encoding uniquely represents the number range, M is invertible over the domain.

To compute the encoding $\mathcal{F}(xy)$ of the product, the operator must produce the phase vector $\Theta_{xy} \equiv M(k * l) \bmod 1$. We analyze two pathways for this from inputs Θ_x and Θ_y:

Pathway A: Disentangle First. One effectively inverts the mixing matrix to recover coefficients: $k = M^{-1}\Theta_x$ and $l = M^{-1}\Theta_y$. The product is then computed as $\Theta_{xy} = M(M^{-1}\Theta_x * M^{-1}\Theta_y)$. The operation M^{-1} represents the full cost of decoding the sinusoidal representation into positional digits.

Pathway B: Disentangle Later. Alternatively, one might attempt to compute the result directly from the entangled phases. Any bilinear operation on the inputs can be expressed via the Kronecker product $\Theta_x \otimes_K \Theta_y$. Substituting the linear forms yields:

$$\Theta_x \otimes_K \Theta_y = (Mk) \otimes_K (Ml) = (M \otimes_K M)(k \otimes_K l) \tag{8}$$

The vector $k \otimes_K l$ contains all cross-terms $k_i l_j$. To construct the convolution h, one must sum all subsets of these cross-terms where $i + j = \tau$. However, the term $\Theta_x \otimes_K \Theta_y$ does not provide direct access to $k_i l_j$, only linear combinations weighted by the expanded mixing matrix $M \otimes_K M$.

Isolating the necessary convolution terms from the bilinear expansion requires inverting this mixing process. This removal $(M \otimes_K M)^{-1} = M^{-1} \otimes_K M^{-1}$ of the cross-term redundancies is therefore computationally at least as expensive as the initial decoding M^{-1}. Moreover, under finite precision, the condition number satisfies $\kappa(M \otimes_K M) = \kappa(M)^2$ with $\kappa(M) \geq 1$, which means that postponing disentanglement amplifies quantization errors.

Since both pathways require inverting the linear mixing M, there exists no shortcut in the sinusoidal domain. Any correct operator $\otimes$ must inherently learn the multi-stage procedure: (1) a non-local decoding of the sinusoidal inputs into internal coefficient sequences for x and y, (2) a convolution of these sequences, followed by (3) a carry propagation step, and finally (4) a re-encoding of the result into the sinusoidal format. □

The preceding proposition demonstrates that performing multiplication in sinusoidal encoding space requires a transformation that is both computationally intensive and prone to precision errors. Any network implementing such an operation is forced to first decode, then calculate, and finally re-encode the encoding. This leads us to conclude that sinusoidal encodings alone are not well-suited as a general purpose number representation.

Potential improvements to sinusoidal encoding To address the aforementioned difficulties of performing multiplication in sinusoidal encoding space, we experimented with applying a logarithmic transformation of the input values before encoding them. In logarithmic space, multiplication reduces to component-wise multiplication, following from the identity $\ln(x_1 x_2) = \ln x_1 + \ln x_2$ and Lemma 4.2.

However, this conversion to a logarithmic space trades one homomorphism for another: multiplication becomes Hadamard-linear, but addition no longer admits a simple local rule, which is a well-known drawback of logarithmic number systems (Chugh & Parhami, 2013; Haselman et al., 2005). Computing $\mathcal{F}_{\log}(x_1 + x_2)$ from $\mathcal{F}_{\log}(x_1)$ and $\mathcal{F}_{\log}(x_2)$ requires learning an effective *exp–sum–log* transformation, reintroducing the same aliasing and inversion difficulties as discussed in Proposition 4.3. Consequently, some operations are easiest to learn in linear space and others in log space. One could simultaneously encode both spaces and use routing mechanisms, such as mixture-of-experts, to enable models to selectively process either encoding and indicate the correct space for decoding. However, our attempts to build such a system were unsuccessful.

5. BitTokens

Guided by the desiderata introduced in Section 3, we propose BitTokens, a novel numeric encoding algorithm. BitTokens uses a dedicated, learnable [NUM] token to which a numeric encoding is added that is based on the IEEE 754 double-precision binary floating-point format (i.e. `float64`) (IEEE, 1985; 2008; 2019). The floating-point

format writes a signed real value v as

$$v = (-1)^s \big(1 + \sum_{i=1}^{52} b_{52-i} 2^{-i}\big) \times 2^{E-1023}, \qquad (9)$$

with $s \in \{0, 1\}$ denoting the sign bit, $E \in \{0, \ldots, 2047\}$ the 11-bit exponent field offset by 1023, and $b_j \in \{0, 1\}$ for $j = 0, \ldots, 51$ the 52 significand bits.

Each bit is mapped to a dimension of the encoding vector, satisfying D1 and D3. The resulting 64-dimensional number encoding provides a representational range of $[2.23 \times 10^{-308}, 1.8 \times 10^{308}]$ with 15–17 significant decimal digits, satisfying D2 and D4. Additionally, it supports special values such as ± 0, $\pm\infty$, and NaN.

Encoding construction: The binary vector of a number can be efficiently constructed via type reinterpretation and bit shifts. To allow for the learning of more efficient division algorithms, we also concatenate the binary representation of the number with a binary representation of its reciprocal value. Scaling the bit vector to $[-1, 1]$ yields unit RMS norm inputs, satisfying D5. We then zero-pad the resulting encoding to match the network's embedding size and then add the vector to the learned [NUM] token embedding. Using raw bit values ensures numerical stability, satisfying D6.

Decoding and loss computation: During next token prediction, the language model outputs a [NUM] token to indicate when it is predicting a number. Then the last hidden state that was used to predict the [NUM] token is passed through a dedicated number head, predicting the binary encoding vector. The number head consists of a linear layer followed by a sigmoid activation, with a fixed decision threshold of 0.5 generating the binary vector representation while increasing robustness to prediction noise, thus satisfying D8. During training, computing a regression loss directly on the reconstructed number from the bit vector is infeasible due to the magnitude of potential values as well as the thresholding operations involved in the process. We therefore employ a bit-wise binary cross entropy loss (BCE) and use equal weighting for each dimension. This does not strictly satisfy condition D7, as illustrated by the predictions $\hat{y}_1 = 8 = 0b1000$ and $\hat{y}_2 = 3 = 0b0011$ for the label $y = 7 = 0b0111$. Although $\hat{y}_1$ is numerically closer to y, it incurs a higher loss than $\hat{y}_2$. In practice, we find that the model is able to account for the structured discontinuities in the target vector, and equal bit weighting further improves performance by encouraging sufficient focus on the more difficult low-significance bits.

Arithmetic properties: Our encoding possesses several properties which ease the learning of mathematical operators, satisfying D9. First, originating from Leibniz's introduction of binary arithmetic (Leibniz (1703)), researchers have developed many efficient algorithms for binary addition and multiplication for modern computing hardware that are compatible with IEEE 754 (Booth, 1951; Wallace, 1964; Brent & Kung, 1982; Kogge & Stone, 2009; Brent & Zimmermann, 2010), Crucially, because each bit is represented independently in our encoding, models can learn algorithms by directly operating upon our BitTokens. As Proposition 4.3 shows, this is not possible with sinusoidal encodings as any multiplication algorithm must first decode, then compute, and finally re-encode the representations.

Second, the IEEE 754 structure separates values into a logarithmic exponent and a linear significand. The simplest algorithm for addition aligns significands by exponent difference and then adds or subtracts them. Multiplication is also simple as exponents are directly added, significands are multiplied, and the sign is determined by an XOR operation. The direct accessibility of individual bits simplifies the network's ability to learn such algorithms.

Third, bit-wise arithmetic over $\mathbb{Z}_2$ results in coefficient-wise operations reducing to Boolean gates:

$$(x \cdot y) \bmod 2 = x \wedge y, \quad (x + y) \bmod 2 = x \oplus y \quad (10)$$

This simplifies the calculations needed for arithmetic.

Finally, calculations using bits can be parallelized across multiple dimensions of the encoding, reducing the number of sequential steps needed and increasing parameter efficiency for learning algorithms.

6. Comparing BitTokens to other tokenizers

Experimental setup We quantify the impact of different tokenization schemes for numeracy in experiments using nanoGPT-2 models (Jordan et al., 2024a). The use of these small language models allows us to train models from scratch and conduct a diverse set of experiments in a controlled environment, as suggested by Allen-Zhu (2024). A full list of architectural details and hyperparameters is included in Appendix D.1. We use the same number tasks and datasets as in Section 2, generating 30M unique training samples of each task. Simultaneously, we include the FineWeb 10B dataset to model training dynamics with text (Penedo et al., 2024).

We compare BitTokens to traditional single digit and triple digit (subword) tokenizers, as well as xVal and FoNE. To enable xVal to process the large number range in our dataset, we rescale the inputs logarithmically instead of linearly to the range of [-5, 5]. FoNE only encodes the magnitude of the number, thus for negative numbers, a $[-]$ token is added before the absolute number encoding. We use 17 integer and 32 fraction frequencies with base $b = 10$.

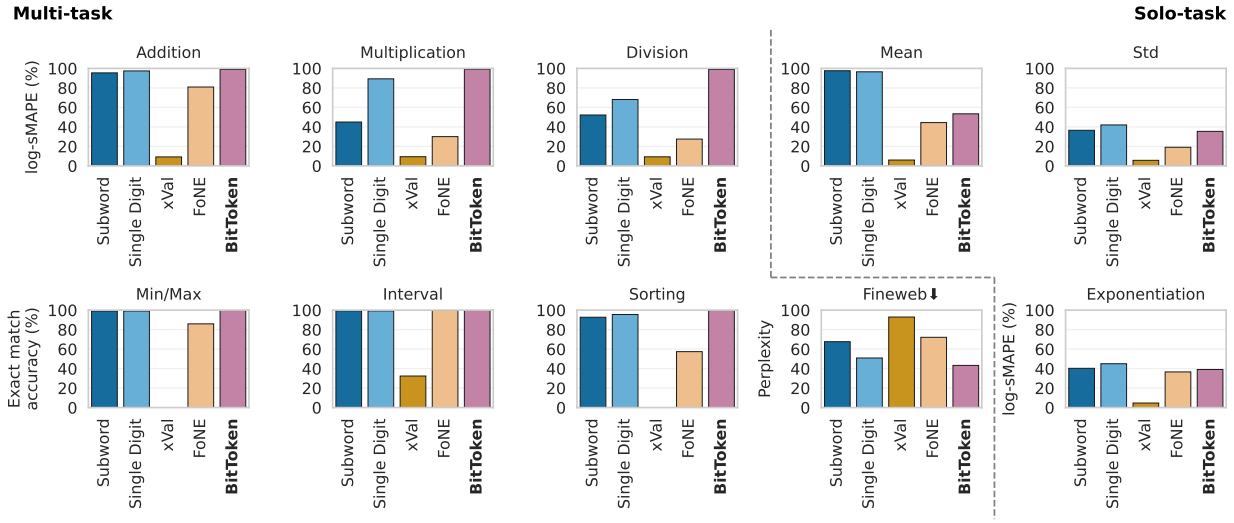

Figure 4. Our BitTokens outperform all other methods in the multi-task setting and is the superior single-token strategy for the multi-step tasks. Between the two multi-token strategies, single digit tokenization performs best, albeit with the highest token cost.

Model training with curriculum learning and dynamic task balancing Since each task category contains both easy and difficult problems, we observe that the performance of small language models, regardless of their tokenization method, can be improved by strategically choosing the order of training samples. We address this by defining a difficulty metric for each problem and employing a curriculum learning strategy with progressive difficulty thresholds, preview sampling, and adaptive advancement criteria, the details of which can be found in Appendix D.3.

The goal of our experiments is to train a model that can learn all ten tasks simultaneously, a setup we call multi-task. During multi-task training, we find that assigning an equal token budget to each of the nine numeracy plus language tasks yields suboptimal performance. This is due to varying task difficulties and their corresponding imbalanced impact on the overall loss. To address this, we dynamically control the composition of each minibatch. An increased sampling probability is assigned to tasks on which the model performs worse. Additional details and discussion of the dynamic task rebalancing are included in Appendix D.4.

We find that the exponentiation, mean, and standard deviation tasks are intrinsically difficult for small language models. We attribute this to the fact that solving these tasks requires sequential application of multiple arithmetic operations. While dynamic rebalancing improves overall performance, a disproportionate token budget would be assigned to these three tasks, preventing convergence on the remaining tasks as shown in Table 14. For this reason, we conduct multi-task experiments on the comparison and single-step calculation tasks plus text. For exponentiation, mean, and standard deviation, we report the solo-task performance.

Results The results of our experiments are shown in Figure 4. Multi-task results show that xVal performs poorly on all tasks, primarily due to its limited precision in representing both input and output. While FoNE is able to learn addition, it struggles with multiplication and division as predicted in Section 4. Among the multi-token strategies, single-digit embeddings consistently outperform subword embeddings. Finally, our BitToken method outperforms all other methods and achieves near-perfect performance on comparison and single-step calculation tasks. Low perplexity scores show that language understanding is not impacted.

Solo-task results indicate that all models struggle with computing standard deviation and exponentiation. Notably, for the mean task, single digit and subword tokenizer methods outperform the single-token methods. We attribute this advantage to the fact that multi-token methods generate answers over multiple forward passes. These models can refine their answers one digit at a time, making it possible to learn iterative algorithms. In contrast, single-token methods need to perform the same work in a single step. While such a built-in iterative behavior can be beneficial in some cases, it also substantially increases computational costs and generation time for simpler tasks, as shown in Table 5. The ablations in Appendix E.3 demonstrate the effectiveness of base-2 encodings over base-10, the benefit of appending the reciprocal, and that curriculum learning substantially boost performance for all methods.

7. Discussion and conclusion

Single-token number representations efficiently encode numerical information in language models. This could reduce the dependency of current frontier LLMs on excessive

amounts of reasoning tokens to solve arithmetic problems while simultaneously reducing the amount of tokens needed to encode numbers. We substantially advance this promising line of research by introducing a set of nine desiderata that ensure a number encoding is efficient, trainable, and effective. Based on these, we propose BitTokens, overcoming the drawbacks of existing single-token approaches.

Our study exclusively evaluates BitTokens on small language models. Although our experiments show that BitTokens integrate well with text during next-token prediction, incorporating them into larger models with broader pretraining data would allow for a more holistic evaluation of their capabilities. Questions include whether BitTokens enhance the ability of LLMs to memorize and recite numerical facts and the interaction with text in math word problems. Moreover, we do not fully outline the steps required to integrate BitTokens in production-level LLMs. These include efficient strategies to robustly identify and parse numbers in input text, accounting for different arithmetic notations, and ensuring models output the correct level of precision for a given context and respect formatting when appropriate, potentially using dedicated [`INT`] and [`FLOAT`] tokens.

While our BitTokens aim to replace excessively long reasoning chains for simple mathematical calculations, reasoning and single-token strategies are not mutually exclusive. Combining them could further improve LLM capabilities on the most complicated problems. By enabling efficient and accurate calculations on intermediate steps, more tokens can be dedicated to logical reasoning, expanding the complexity of problems language models can solve.

Acknowledgements

This work was partially funded by ERC Grant Deep4MI (Grant No. 884622). The authors gratefully acknowledge the scientific support and HPC resources provided by the Erlangen National High Performance Computing Center (NHR@FAU) of the Friedrich-Alexander-Universitaet Erlangen-Nuernberg (FAU) under the NHR project b247bb. NHR funding is provided by federal and Bavarian state authorities. NHR@FAU hardware is partially funded by the DFG under project 440719683. Martin J. Menten is funded by the German Research Foundation under project 532139938.

Impact Statement

This paper presents work whose goal is to advance the field of Machine Learning. There are many potential societal consequences of our work, none which we feel must be specifically highlighted here.

References

Agarwal, S., Ahmad, L., Ai, J., Altman, S., Applebaum, A., Arbus, E., Arora, R. K., Bai, Y., Baker, B., Bao, H., et al. gpt-oss-120b & gpt-oss-20b model card. *arXiv preprint arXiv:2508.10925*, 2025.

Ahn, J., Verma, R., Lou, R., Liu, D., Zhang, R., and Yin, W. Large language models for mathematical reasoning: Progresses and challenges. In *Proceedings of the 18th Conference of the European Chapter of the Association for Computational Linguistics: Student Research Workshop*, pp. 225–237, 2024.

AI4Science, M. R. and Quantum, M. A. The impact of large language models on scientific discovery: a preliminary study using GPT-4. *arXiv preprint arXiv:2311.07361*, 2023.

Akhtar, M., Shankarampeta, A., Gupta, V., Patil, A., Cocarascu, O., and Simperl, E. Exploring the numerical reasoning capabilities of language models: A comprehensive analysis on tabular data. In *The 2023 Conference on Empirical Methods in Natural Language Processing*, 2023.

Alberts, M., Gabrieli, G., and Morales, I. E. Interleaving text and number embeddings to solve mathemathics problems. In *The 4th Workshop on Mathematical Reasoning and AI at NeurIPS'24*, 2024. URL https://openreview.net/forum?id=8cNJyqs45T.

Allen-Zhu, Z. ICML 2024 Tutorial: Physics of Language Models, July 2024. Project page: https://physics.allen-zhu.com/.

Baeumel, T., Genabith, J. V., and Ostermann, S. The lookahead limitation: Why multi-operand addition is hard for LLMs. In Belinkov, Y., Mueller, A., Kim, N., Mohebbi, H., Chen, H., Arad, D., and Sarti, G. (eds.), *Proceedings of the 8th BlackboxNLP Workshop: Analyzing and Interpreting Neural Networks for NLP*, pp. 250–262, Suzhou, China, November 2025. Association for Computational Linguistics. ISBN 979-8-89176-346-3. doi: 10.18653/v1/2025.blackboxnlp-1.15. URL https://aclanthology.org/2025.blackboxnlp-1.15/.

Booth, A. D. A signed binary multiplication technique. *The Quarterly Journal of Mechanics and Applied Mathematics*, 4(2):236–240, 1951.

Brent, R. P. and Kung, H. T. A regular layout for parallel adders. *IEEE transactions on Computers*, 100(3):260–264, 1982.

Brent, R. P. and Zimmermann, P. *Modern computer arithmetic*, volume 18. Cambridge University Press, 2010.

Charton, F. Learning the greatest common divisor: explaining transformer predictions. In Kim, B., Yue, Y., Chaudhuri, S., Fragkiadaki, K., Khan, M., and Sun, Y. (eds.), *International Conference on Representation Learning*, volume 2024, pp. 50714–50734, 2024. URL https://iclr.cc/virtual/2024/poster/18284.

Chen, C.-C., Huang, H.-H., Takamura, H., and Chen, H.-H. Numeracy-600k: Learning numeracy for detecting exaggerated information in market comments. In *Proceedings of the 57th Annual Meeting of the Association for Computational Linguistics*, pp. 6307–6313, 2019.

Chiang, W.-L., Zheng, L., Sheng, Y., Angelopoulos, A. N., Li, T., Li, D., Zhu, B., Zhang, H., Jordan, M., Gonzalez, J. E., et al. Chatbot arena: An open platform for evaluating LLMs by human preference. In *Forty-first International Conference on Machine Learning*, 2024.

Chugh, M. and Parhami, B. Logarithmic arithmetic as an alternative to floating-point: A review. In *2013 Asilomar Conference on Signals, Systems and Computers*, pp. 1139–1143, 2013.

Cobbe, K., Kosaraju, V., Bavarian, M., Chen, M., Jun, H., Kaiser, L., Plappert, M., Tworek, J., Hilton, J., Nakano, R., et al. Training verifiers to solve math word problems. *arXiv preprint arXiv:2110.14168*, 2021.

Comanici, G., Bieber, E., Schaekermann, M., Pasupat, I., Sachdeva, N., Dhillon, I., Blistein, M., Ram, O., Zhang, D., Rosen, E., et al. Gemini 2.5: Pushing the frontier with advanced reasoning, multimodality, long context, and next generation agentic capabilities. *arXiv preprint arXiv:2507.06261*, 2025.

Cui, H., Shamsi, Z., Cheon, G., Ma, X., Li, S., Tikhanovskaya, M., Norgaard, P. C., Mudur, N., Plomecka, M. B., Raccuglia, P., et al. Curie: Evaluating LLMs on multitask scientific long-context understanding and reasoning. In *The Thirteenth International Conference on Learning Representations*, 2025.

Dao, T. FlashAttention-2: Faster attention with better parallelism and work partitioning. In *The Twelfth International Conference on Learning Representations*, 2024.

DeepSeek-AI. DeepSeek-V3 technical report, 2024. URL https://arxiv.org/abs/2412.19437.

Fang, X., Xu, W., Tan, F. A., Hu, Z., Zhang, J., Qi, Y., Sengamedu, S. H., and Faloutsos, C. Large language models (LLMs) on tabular data: Prediction, generation, and understanding - a survey. *Transactions on Machine Learning Research*, 2024. ISSN 2835-8856. URL https://openreview.net/forum?id=IZnrCGF9WI.

Flores, B. E. A pragmatic view of accuracy measurement in forecasting. *Omega*, 14(2):93–98, 1986.

Gao, L., Madaan, A., Zhou, S., Alon, U., Liu, P., Yang, Y., Callan, J., and Neubig, G. PAL: program-aided language models. In *Proceedings of the 40th International Conference on Machine Learning*, pp. 10764–10799, 2023.

Gardner, J., Perdomo, J. C., and Schmidt, L. Large scale transfer learning for tabular data via language modeling. *Advances in Neural Information Processing Systems*, 37: 45155–45205, 2024.

Golkar, S., Pettee, M., Eickenberg, M., Bietti, A., Cranmer, M., Krawezik, G., Lanusse, F., McCabe, M., Ohana, R., Parker, L. H., et al. xval: A continuous number encoding for large language models. In *NeurIPS 2023 AI for Science Workshop*, 2023.

Gou, Z., Shao, Z., Gong, Y., Shen, Y., Yang, Y., Huang, M., Duan, N., and Chen, W. ToRA: A tool-integrated reasoning agent for mathematical problem solving. In *The Twelfth International Conference on Learning Representations*, 2024.

Gu, Y., Shu, Y., Yu, H., Liu, X., Dong, Y., Tang, J., Srinivasa, J., Latapie, H., and Su, Y. Middleware for llms: Tools are instrumental for language agents in complex environments. In *Proceedings of the 2024 Conference on Empirical Methods in Natural Language Processing*, pp. 7646–7663, 2024.

Hager, P., Jungmann, F., Holland, R., Bhagat, K., Hubrecht, I., Knauer, M., Vielhauer, J., Makowski, M., Braren, R., Kaissis, G., and Rueckert, D. Evaluation and mitigation of the limitations of large language models in clinical decision-making. *Nature Medicine*, 30(9):2613–2622, 2024.

Han, H., Xu, J., Zhou, M., Shao, Y., Han, S., and Zhang, D. LUNA: language understanding with number augmentations on transformers via number plugins and pre-training. *arXiv preprint arXiv:2212.02691*, 2022.

Hao, S., Sukhbaatar, S., Su, D., Li, X., Hu, Z., Weston, J. E., and Tian, Y. Training large language models to reason in a continuous latent space. In *Workshop on Reasoning and Planning for Large Language Models*, 2025. URL https://openreview.net/forum?id=KrWSrrYGpT.

Haselman, M., Beauchamp, M., Wood, A., Hauck, S., Underwood, K., and Hemmert, K. S. A comparison of floating point and logarithmic number systems for FPGAs. In *13th Annual IEEE Symposium on Field-Programmable Custom Computing Machines (FCCM'05)*, pp. 181–190. IEEE, 2005.

He-Yueya, J., Poesia, G., Wang, R., and Goodman, N. Solving math word problems by combining language models with symbolic solvers. In *The 3rd Workshop on Mathematical Reasoning and AI at NeurIPS'23*, 2023.

Hegselmann, S., Buendia, A., Lang, H., Agrawal, M., Jiang, X., and Sontag, D. Tabllm: Few-shot classification of tabular data with large language models. In *International conference on artificial intelligence and statistics*, pp. 5549–5581. PMLR, 2023.

IEEE. IEEE Standard for Binary Floating-Point Arithmetic. ANSI/IEEE Std 754-1985, 1985.

IEEE. IEEE Standard for Floating-Point Arithmetic. IEEE Std 754-2008, 2008.

IEEE. IEEE Standard for Floating-Point Arithmetic. IEEE Std 754-2019, 2019.

Jordan, K., Bernstein, J., Rappazzo, B., @fernbear.bsky.social, Vlado, B., Jiacheng, Y., Cesista, F., Koszarsky, B., and @Grad62304977. modded-nanogpt: Speedrunning the nanoGPT baseline, 2024a. URL https://github.com/KellerJordan/modded-nanogpt.

Jordan, K., Jin, Y., Boza, V., Jiacheng, Y., Cesista, F., Newhouse, L., and Bernstein, J. Muon: An optimizer for hidden layers in neural networks, 2024b. URL https://kellerjordan.github.io/posts/muon/.

Kogge, P. M. and Stone, H. S. A parallel algorithm for the efficient solution of a general class of recurrence equations. *IEEE transactions on computers*, 100(8):786–793, 2009.

Kwa, T., West, B., Becker, J., Deng, A., Garcia, K., Hasin, M., Jawhar, S., Kinniment, M., Rush, N., Von Arx, S., Bloom, R., Broadley, T., Du, H., Goodrich, B., Jurkovic, N., Miles, L., Nix, S., Lin, T., Parikh, N., Rein, D., Koba Sato, L. J., Wijk, H., Ziegler, D., Barnes, E., and Chan, L. Measuring ai ability to complete long software tasks. In Belgrave, D., Zhang, C., Lin, H., Pascanu, R., Koniusz, P., Ghassemi, M., and Chen, N. (eds.), *Advances in Neural Information Processing Systems*, volume 38, pp. 92213–92266. Curran Associates, Inc., 2025. URL https://neurips.cc/virtual/2025/loc/san-diego/poster/119302.

Le, H., Wang, Y., Gotmare, A. D., Savarese, S., and Hoi, S. C. H. CodeRL: Mastering code generation through pretrained models and deep reinforcement learning. *Advances in Neural Information Processing Systems*, 35: 21314–21328, 2022.

Lee, N., Sreenivasan, K., Lee, J. D., Lee, K., and Papailiopoulos, D. Teaching arithmetic to small transformers. In *International Conference on Learning Representations*. ICLR, 2024.

Leibniz, G. W. Explication de l'arithmétique binaire, qui se sert des seuls caractères 0 et 1, avec des remarques sur son utilité, et sur ce qu'elle donne le sens des anciennes figures chinoises de fohy. *Acta Eruditorum*, pp. 85–89, 1703.

Li, H., Chen, X., Xu, Z., Li, D., Hu, N., Teng, F., Li, Y., Qiu, L., Zhang, C. J., Qing, L., and Chen, L. Exposing numeracy gaps: A benchmark to evaluate fundamental numerical abilities in large language models. In Che, W., Nabende, J., Shutova, E., and Pilehvar, M. T. (eds.), *Findings of the Association for Computational Linguistics: ACL 2025*, pp. 20004–20026, Vienna, Austria, July 2025. Association for Computational Linguistics. ISBN 979-8-89176-256-5. doi: 10.18653/v1/2025.findings-acl.1026. URL https://aclanthology.org/2025.findings-acl.1026/.

Lightman, H., Kosaraju, V., Burda, Y., Edwards, H., Baker, B., Lee, T., Leike, J., Schulman, J., Sutskever, I., and Cobbe, K. Let's verify step by step. In *The Twelfth International Conference on Learning Representations*, 2023.

Lindsey, J., Gurnee, W., Ameisen, E., Chen, B., Pearce, A., Turner, N. L., Citro, C., Abrahams, D., Carter, S., Hosmer, B., Marcus, J., Sklar, M., Templeton, A., Bricken, T., McDougall, C., Cunningham, H., Henighan, T., Jermyn, A., Jones, A., Persic, A., Qi, Z., Thompson, T. B., Zimmerman, S., Rivoire, K., Conerly, T., Olah, C., and Batson, J. On the biology of a large language model. *Transformer Circuits Thread*, 2025. URL https://transformer-circuits.pub/2025/attribution-graphs/biology.html.

Liu, T., Wang, F., and Chen, M. Rethinking tabular data understanding with large language models. In *Proceedings of the 2024 Conference of the North American Chapter of the Association for Computational Linguistics: Human Language Technologies (Volume 1: Long Papers)*, pp. 450–482, 2024.

McLeish, S., Bansal, A., Stein, A., Jain, N., Kirchenbauer, J., Bartoldson, B., Kailkhura, B., Bhatele, A., Geiping, J., Schwarzschild, A., et al. Transformers can do arithmetic with the right embeddings. *Advances in Neural Information Processing Systems*, 37: 108012–108041, 2024. URL https://neurips.cc/virtual/2024/poster/94565.

Meta. The LLaMA 4 herd: The beginning of a new era of natively multimodal AI innovation. Meta AI Blog,

April 5 2025. URL https://ai.meta.com/blog/llama-4-multimodal-intelligence/.

Mirzadeh, S. I., Alizadeh, K., Shahrokhi, H., Tuzel, O., Bengio, S., and Farajtabar, M. GSM-symbolic: Understanding the limitations of mathematical reasoning in large language models. In *The Thirteenth International Conference on Learning Representations*, 2025. URL https://iclr.cc/virtual/2025/poster/30620.

Nogueira, R., Jiang, Z., and Lin, J. Investigating the limitations of transformers with simple arithmetic tasks. *arXiv preprint arXiv:2102.13019*, 2021.

OpenAI. Introducing GPT-5. OpenAI Blog / Product Release, August 7 2025. URL https://openai.com/index/introducing-gpt-5/.

Parisi, A., Zhao, Y., and Fiedel, N. TALM: Tool augmented language models. *arXiv preprint arXiv:2205.12255*, 2022.

Penedo, G., Kydlíček, H., allal, L. B., Lozhkov, A., Mitchell, M., Raffel, C., Werra, L. V., and Wolf, T. The FineWeb datasets: Decanting the web for the finest text data at scale. In *The Thirty-eight Conference on Neural Information Processing Systems Datasets and Benchmarks Track*, 2024.

Qu, C., Dai, S., Wei, X., Cai, H., Wang, S., Yin, D., Xu, J., and Wen, J.-r. Tool learning with large language models: a survey. *Frontiers of Computer Science*, 19(8):198343, Jan 2025.

Schick, T., Dwivedi-Yu, J., Dessì, R., Raileanu, R., Lomeli, M., Hambro, E., Zettlemoyer, L., Cancedda, N., and Scialom, T. Toolformer: Language models can teach themselves to use tools. *Advances in Neural Information Processing Systems*, 36:68539–68551, 2023.

Schwartz, E., Choshen, L., Shtok, J., Doveh, S., Karlinsky, L., and Arbelle, A. NumeroLogic: Number encoding for enhanced LLMs' numerical reasoning. In Al-Onaizan, Y., Bansal, M., and Chen, Y.-N. (eds.), *Proceedings of the 2024 Conference on Empirical Methods in Natural Language Processing*, pp. 206–212, Miami, Florida, USA, November 2024. Association for Computational Linguistics. doi: 10.18653/v1/2024.emnlp-main.12. URL https://aclanthology.org/2024.emnlp-main.12/.

Shao, Z., Wang, P., Zhu, Q., Xu, R., Song, J., Bi, X., Zhang, H., Zhang, M., Li, Y., Wu, Y., et al. DeepSeekMath: Pushing the limits of mathematical reasoning in open language models. *arXiv preprint arXiv:2402.03300*, 2024.

Shen, R., Bubeck, S., Eldan, R., Lee, Y. T., Li, Y., and Zhang, Y. Positional description matters for transformers arithmetic. *arXiv preprint arXiv:2311.14737*, 2023.

Singh, A. K. and Strouse, D. Tokenization counts: the impact of tokenization on arithmetic in frontier LLMs. *arXiv preprint arXiv:2402.14903*, 2024.

Singhal, P., Goyal, T., Xu, J., and Durrett, G. A long way to go: Investigating length correlations in RLHF. In *First Conference on Language Modeling*, 2024. URL https://openreview.net/forum?id=G8LaO1P0xv.

Skean, O., Arefin, M. R., and Shwartz-Ziv, R. Does representation matter? exploring intermediate layers in large language models. In *Workshop on Machine Learning and Compression, NeurIPS*, 2024.

Snell, C., Lee, J., Xu, K., and Kumar, A. Scaling llm test-time compute optimally can be more effective than scaling parameters for reasoning. In Yue, Y., Garg, A., Peng, N., Sha, F., and Yu, R. (eds.), *International Conference on Learning Representations*, volume 2025, pp. 10131–10165, 2025. URL https://openreview.net/forum?id=4FWAwZtd2n.

Su, J., Ahmed, M., Lu, Y., Pan, S., Bo, W., and Liu, Y. Roformer: Enhanced transformer with rotary position embedding. *Neurocomputing*, 568(C), February 2024. ISSN 0925-2312. doi: 10.1016/j.neucom.2023.127063. URL https://doi.org/10.1016/j.neucom.2023.127063.

Team, K., Bai, Y., Bao, Y., Chen, G., Chen, J., Chen, N., Chen, R., Chen, Y., Chen, Y., Chen, Y., et al. Kimi K2: Open agentic intelligence. *arXiv preprint arXiv:2507.20534*, 2025.

Wallace, C. S. A suggestion for a fast multiplier. *IEEE Transactions on Electronic Computers*, EC-13(1):14–17, 1964.

Wang, X., Wei, J., Schuurmans, D., Le, Q. V., Chi, E. H., Narang, S., Chowdhery, A., and Zhou, D. Self-consistency improves chain of thought reasoning in language models. In *The Eleventh International Conference on Learning Representations*, 2023.

Wang, Y., Ma, X., Zhang, G., Ni, Y., Chandra, A., Guo, S., Ren, W., Arulraj, A., He, X., Jiang, Z., Li, T., Ku, M., Wang, K., Zhuang, A., Fan, R., Yue, X., and Chen, W. MMLU-pro: A more robust and challenging multi-task language understanding benchmark. In *The Thirty-eight Conference on Neural Information Processing Systems Datasets and Benchmarks Track*, 2024a.

Wang, Z., Zhang, H., Li, C.-L., Eisenschlos, J. M., Perot, V., Wang, Z., Miculicich, L., Fujii, Y., Shang, J., Lee, C.-Y., and Pfister, T. Chain-of-table: Evolving tables in the reasoning chain for table understanding. In *The Twelfth International Conference on Learning Representations*,

2024b. URL https://openreview.net/forum?id=4L0xnS4GQM.

Wei, J., Wang, X., Schuurmans, D., Bosma, M., Xia, F., Chi, E., Le, Q. V., Zhou, D., et al. Chain-of-thought prompting elicits reasoning in large language models. *Advances in neural information processing systems*, 35:24824–24837, 2022.

Yang, A., Li, A., Yang, B., Zhang, B., Hui, B., Zheng, B., Yu, B., Gao, C., Huang, C., Lv, C., et al. Qwen3 technical report. *arXiv preprint arXiv:2505.09388*, 2025a.

Yang, H., Hu, Y., Kang, S., Lin, Z., and Zhang, M. Number cookbook: Number understanding of language models and how to improve it. In *The Thirteenth International Conference on Learning Representations*, 2025b.

Yao, S., Yu, D., Zhao, J., Shafran, I., Griffiths, T., Cao, Y., and Narasimhan, K. Tree of thoughts: Deliberate problem solving with large language models. *Advances in neural information processing systems*, 36:11809–11822, 2023.

Yeo, E., Tong, Y., Niu, X., Neubig, G., and Yue, X. Demystifying long chain-of-thought reasoning in LLMs. In *ICLR 2025 Workshop on Navigating and Addressing Data Problems for Foundation Models*, 2025. URL https://openreview.net/forum?id=AgtQlhMQ0V.

Zhang, B., Zhou, K., Wei, X., Zhao, X., Sha, J., Wang, S., and Wen, J.-R. Evaluating and improving tool-augmented computation-intensive math reasoning. In *Thirty-seventh Conference on Neural Information Processing Systems Datasets and Benchmarks Track*, 2023.

Zhang, W., Wan, C., Zhang, Y., Cheung, Y.-m., Tian, X., Shen, X., and Ye, J. Interpreting and improving large language models in arithmetic calculation. In *Proceedings of the 41st International Conference on Machine Learning*, pp. 59932–59950, 2024.

Zhang, X., Luo, S., Zhang, B., Ma, Z., Zhang, J., Li, Y., Li, G., Yao, Z., Xu, K., Zhou, J., et al. Tablellm: Enabling tabular data manipulation by llms in real office usage scenarios. In *Findings of the Association for Computational Linguistics: ACL 2025*, pp. 10315–10344, 2025.

Zhou, T., Fu, D., Soltanolkotabi, M., Jia, R., and Sharan, V. FoNE: Precise single-token number embeddings via fourier features. In *The Fourteenth International Conference on Learning Representations*, 2026. URL https://openreview.net/forum?id=g0vtWmwDDh.

A. Reproducibility

We took several steps to ensure our results are reproducible. Dataset construction is specified in Section 2, with the exact number-sampling scheme and the task difficulty metric detailed in Appendix B.2 and Appendix B.3. The full experimental setup for the BitToken method and all baselines is described in Section 6, with model architectures and hyperparameter configurations in Appendix D, and additional details for curriculum learning and multi-task training in Appendix D.3 and Appendix D.4. Our code is available at `https://github.com/KreitnerL/BitTokens`. This repository includes code for the frontier-model benchmark (including evaluation scripts), the BitToken method, and for running the experiments. These materials provide the code and configuration files needed to reproduce the reported experiments and regenerate the results referenced in the paper.

B. Benchmarking dataset

B.1. Tasks

B.1.1. Comparing numbers

The most elementary numeracy task is comparing two random numbers, n_1 and n_2. As this task is near-perfectly solved by modern LLMs, we increase the difficulty to multiple operands.

Determining the minimum and maximum

Determining the minimum or maximum of a list of numbers is in essence a series of number comparisons where one number must be held in memory. Each list is comprised of l floats, with $l \in \{2, 3, 4, 5\}$. We use the following phrasings:

MinMax phrasing

```
What is the maximum of the list [n1, n2]
What is the minimum of the list [n1, n2, n3, n4, n5]
```

Our system prompt is:

MinMax system prompt

```
You are an expert in numeracy.  For each problem, output only valid JSON in
this format:
"answer":  <numeric_answer>
Do not explain, show steps, or add any extra text.  Do not use code blocks
to output the answer.
DO NOT CALL ANY external APIs or use ANY external tool to solve the problem.
DO NOT USE a calculator tool.  DO NOT USE python.  DO NOT USE Wolfram Alpha.
The answer must be a single number, exactly as it appears in the list.
```

We evaluate by calculating the exact string match accuracy of the answer.

Interval assignment

Determining if a number falls within an interval can be achieved by a series of pairwise comparisons, where two numbers must be held in memory. Each list is comprised of l floats, with $l \in \{2, 3, 4, 5\}$. We use the following phrasing:

Interval phrasing

```
What interval does x=n belong to?  A: x < n1, B: n1 <= x < n2, C: n2 <= x
```

Our system prompt is:

Interval system prompt

```
You are an expert in numeracy.  For each problem, output only valid JSON in
this format:
"answer":  <interval_multiple_choice_answer>
Do not explain, show steps, or add any extra text.  Do not use code blocks
to output the answer.
DO NOT CALL ANY external APIs or use ANY external tool to solve the problem.
DO NOT USE a calculator tool.  DO NOT USE python.  DO NOT USE Wolfram Alpha.
The answer must be one of the following:  A, B, C, D, E, F.
```

We evaluate by calculating the exact string match accuracy of the answer.

List sorting

Sorting a list of numbers is in requires more numbers to be held in memory (depending on the "algorithm" used by the LLM). Each list consists of l floats, with $l \in \{2, 3, 4, 5\}$. We use the following phrasing:

Sorting phrasing

Sort the list [n_1, n_2, n_3, n_4, n_5] in ascending order.
Sort the list [n_1, n_2, n_3] in descending order.

Our system prompt is:

Sorting system prompt

```
You are an expert in numeracy.  For each problem, output only valid JSON in
this format:
"answer":  <sorted_list>
Do not explain, show steps, or add any extra text.  Do not use code blocks
to output the answer.
DO NOT CALL ANY external APIs or use ANY external tool to solve the problem.
DO NOT USE a calculator tool.  DO NOT USE python.  DO NOT USE Wolfram Alpha.
The answer must be a list of numbers.
```

We evaluate by calculating the exact string match accuracy of the answer.

B.1.2. Single-step arithmetic

We test both addition and subtraction capabilities in the addition task, but separate multiplication and division as the generation of the multiplicative inverse is not trivial. We use the following phrasing:

Single-step arithmetic phrasing

What is n_1 + n_2?
What is n_1 - n_2?
What is n_1 * n_2?
What is n_1 / n_2?

Our system prompt is:

Single-step arithmetic system prompt

```
You are an expert in numeracy.  Return exactly one valid JSON object in this
format:
"answer":  <numeric_answer>
Do not explain, show steps, or add any extra text.  Do not use code blocks
to output the answer.
DO NOT CALL ANY external APIs or use ANY external tool to solve the problem.
DO NOT USE a calculator tool.  DO NOT USE python.  DO NOT USE Wolfram Alpha.
If the answer is not an integer, give it as a decimal (not a fraction),
rounded to at most 15 significant digits.
```

We use $\log\text{-sMAPE}$ and exact match accuracy as metrics.

B.1.3. Multi-step arithmetic

The exponentiation task includes both positive and negative exponents as well as float exponents, thus testing both power and root operations. We also test the ability to calculate both the mean and the standard deviation. Calculating the mean requires adding all numbers in the list and then dividing by the length of the list. Calculating the standard deviation requires calculating the mean of the list, then calculating the average difference between the mean and each element squared, and then taking the square root of that average. We use a single set of number lists for both tasks. Each list comprises l floats, with $l \in \{2, 3, 4, 5\}$. We use the following phrasing:

Mean, Std, and exponentiation phrasing

What is the mean of the list [n_1, n_2, n_3]?
What is the std of the list [n_1, n_2, n_3, n_4]?
What is n_1 ^ n_2?

Our system prompt is:

Multi-step arithmetic system prompt

```
You are an expert in numeracy.  Return exactly one valid JSON object in this
format:
"answer":  <numeric_answer>
Do not explain, show steps, or add any extra text.  Do not use code blocks
to output the answer.
DO NOT CALL ANY external APIs or use ANY external tool to solve the problem.
DO NOT USE a calculator tool.  DO NOT USE python.  DO NOT USE Wolfram Alpha.
If the answer is not an integer, give it as a decimal (not a fraction),
rounded to at most 15 significant digits.
```

We use $\log\text{-sMAPE}$ and exact match accuracy as metrics.

B.2. Number sampling

We sample all numbers from the interval $[10^{-14}, 10^{15}) \cup \{0\}$ and ensure that the result is in the same interval. For each task, we sample the operands $n \sim \mathcal{U}(10^x, 10^{x+1})$, where $x \sim \mathcal{U}(-14, 15)$. We ensure that all numbers can be represented without loss of information by a `float64` tensor and round all answers to at most 15 significant digits. Further, we ensure that the operation of both numbers does not result in vanishing information. For instance, computing the mean of the list $[10^{14}, 10^{-5}, -10^{14}]$ in python would be evaluated as 0 because the intermediate result $10^{14} + 10^{-5}$ cannot be represented given the limited precision of 15-17 digits.

When used by humans, numbers often occur a reduced number of decimal digits, while full precision is used in scientific and engineering environments. To reflect both use cases, we uniformly sample the number of significant digits of the values

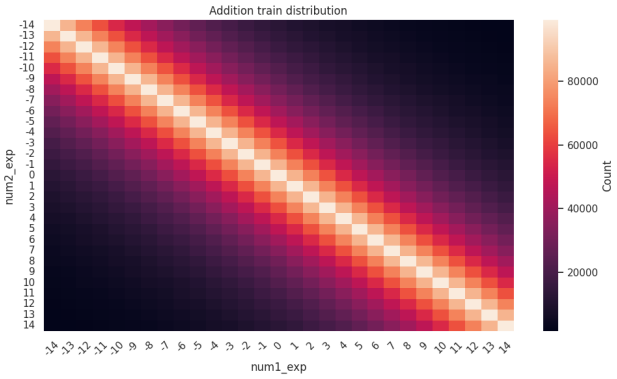

(a) Addition pairs. Operands with similar exponents are oversampled to increase difficulty.

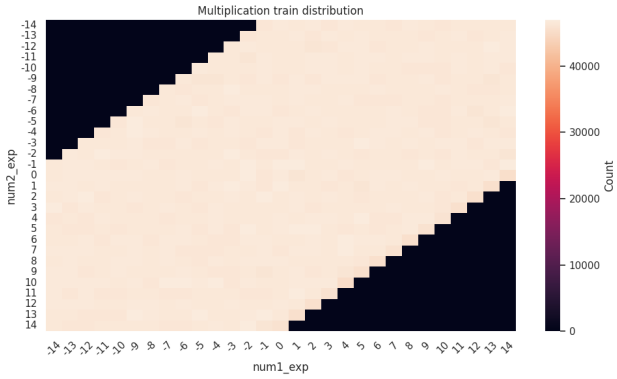

(b) Multiplication pairs.

Figure 5. Magnitude distributions of arithmetic pairs in our dataset.

from a uniform distribution.

For each task, we sample 30M train samples, 10k validation and 10k test samples. In the following, we outline task specific generation parameters.

MinMax / Interval / Sorting We draw the list length $l \in \{2, 3, 4, 5\}$ and the magnitude of the mean of all operands from $x \sim \mathcal{U}(-14, 15)$. We then sample operands for each spread $s \in [\min(13, x - 13), \min(x + 2, 13)]$. This increases the number of samples where the numbers share a common prefix and only differ in few digits, thus increasing difficulty. We then draw $m \sim \mathcal{U}(10^x, 10^{x+1})$ and generate a list of numbers $[n_1, \ldots, n_l],\ n_i \in [m - s, m + s]$ such that $\frac{1}{l}\sum_{i=0}^{l} n_i = m$. We ensure that each list element only has a maximum of $p \sim \mathcal{U}(1, 17)$ significant digits. Because of the limited precision, we cannot guarantee that the mean will be m. We therefore draw 1000 lists and take the one that has the closest mean. We ensure that $\sigma \neq 0$, as well as $m \neq 0$ if $l \in \{2, 4\}$ to avoid trivial samples.

For the MinMax task, we randomly choose whether we require the minimum or the maximum of the list. For the sorting task, we randomly choose whether the list should be sorted ascending or descending. For the interval task, we randomly choose a position index $pos \in [0, \ldots, l]$. We then draw a reference value from the sorted list L:

$$ref \sim \begin{cases} L_0 - 10^s/l & pos = 0 \\ \mathcal{U}(L_{pos-1}, L_{pos}) & 0 < pos < l \\ L_{l-1} + 10^s/l & pos = l \end{cases} \tag{11}$$

Addition A core challenge during addition lies in the carry propagation. If the exponents of the operands are farther apart than the precision limit of `float64`, the answer to the calculation is simply the larger number. We therefore prioritize sampling of cases where both operands are of similar magnitude (see Figure 5a). We sample the combined operand precision $p_{12} \in \mathcal{U}(2, 34)$ from a uniform distribution. We then draw $p_1 \in \text{triangular}(l, l + 1, \min(p_{12} - 1, 17))$ with $l = \lceil \frac{p_{12}}{2} \rceil$ from a triangular distribution and set $p_2 = p_{12} - p_1$. We then round the operands by p_1 and p_2 respectively and randomly swap operands. We choose the individual signs using the following schema: (1) both positive in 40% of cases, (2) only one operand negative in 40% of cases and (3) both negative in 20% of cases. We randomly choose an operator $op \in \{+, -\}$.

Multiplication We handle precision of the operands and their signs similar to the addition task, however, we do not swap the operands as this could result in the product being out of bounds.

Division Similar to addition, we draw the combined precision of the quotient and the divisor and sample their individual precisions. We then compute the dividend from the quotient and divisor. We change signs similar to the addition task, however, we do not swap the operands as this could result in the product being out of bounds.

Exponentiation We draw the exponent x from the interval $[-14, 15)$ and increase the number of samples closer to zero. We

choose base $b \sim \mathcal{U}(10^x, 10^{x-1})$, choose $\xi \in \left[\lceil \frac{10^{-13}}{|x|+1} \rceil, \lfloor \frac{10^{14}}{|x|+1} \rfloor\right]$ and set for all $\xi \notin \{0, 1\}$:

$$exp = \begin{cases} \xi & \xi > 1 \\ 1/\xi & \text{else} \end{cases} \tag{12}$$

This procedure ensures that we only use integer powers and integer roots. If $b > 1$, we randomly set b negative. We also choose the sign of exp randomly.

Mean and standard deviation We generate a list similar to the method described for task MinMax but choose $s \in [\min(13, x-13),\ \min(x+17, 13)]$ since here, a smaller spread would overly simplify the task.

B.3. Problem difficulty

Our experiments show that our small scale transformer models benefit from curriculum learning. To maximize sample efficiency, we manually define a difficulty heuristic that is used for sampling. This avoids inefficient loss based selection. Curriculum training is only used for the most difficult tasks multiplication, division, exponentiation, mean and standard deviation.

Most difficulty heuristics are defined using the digit representation of the operands. In the following, we will describe the difficulty for each task depending on its base. We ensure difficulty $\delta_\tau \in \mathbb{N}_0$.

Multiplication Given the fixed-point number representations of the operands in base-2 or base-10, the difficulty $\delta_{\text{Multiplication}}$ is given by the sum of their non-zero digits. This directly correlates with the number of steps involved to solve the task and the numbers' precision.

Division Similar to Multiplication, the difficulty $\delta_{\text{Multiplication}}$ is given by the sum of the non-zero digits of dividend, divisor and quotient.

Mean For Mean we found the most reliable difficulty metric to be $\delta_{\text{Mean}} = s - x + 15$ with spread s and exponent x of the mean of the list. Intuitively, the difficulty increases for larger spreads. We see a clear drop in performance for all models where $s > x$, that is, where numbers do no longer share any common prefix.

Exponentiation / Standard deviation While the difficulty heuristic for Multiplication, Division and Mean can be derived relatively straightforward, a heuristic for the remaining tasks is a lot harder to define. This is because of their inherent multi-step nature. Each result can be computed using a large variety of different algorithms. For instance, consider the task of computing the standard deviation of a list $L = \{x_1, \ldots, x_N\}$ with mean μ. Possible solutions include $\sqrt{\frac{1}{N}\sum_{i=1}^{N}(x_i - \mu)}$, $\sqrt{\frac{1}{N}\sum_{i=1}^{N} x_i^2 - \mu^2}$, Welford's online algorithm, and many more. We define heuristic δ_{exp} as the product of the number of non-zero digits of each base, exponent, and result and, for simplicity reasons, set $\delta_{\text{Std}} = \delta_{\text{Mean}}$.

B.4. Subsampling

Due to cost constraints we had to select a subset of the full set of 10,000 test samples when evaluating the frontier LLMs. As shown in Figure 6, the benchmark for the frontier LLMs and our BitTokens follow the same difficulty distribution.

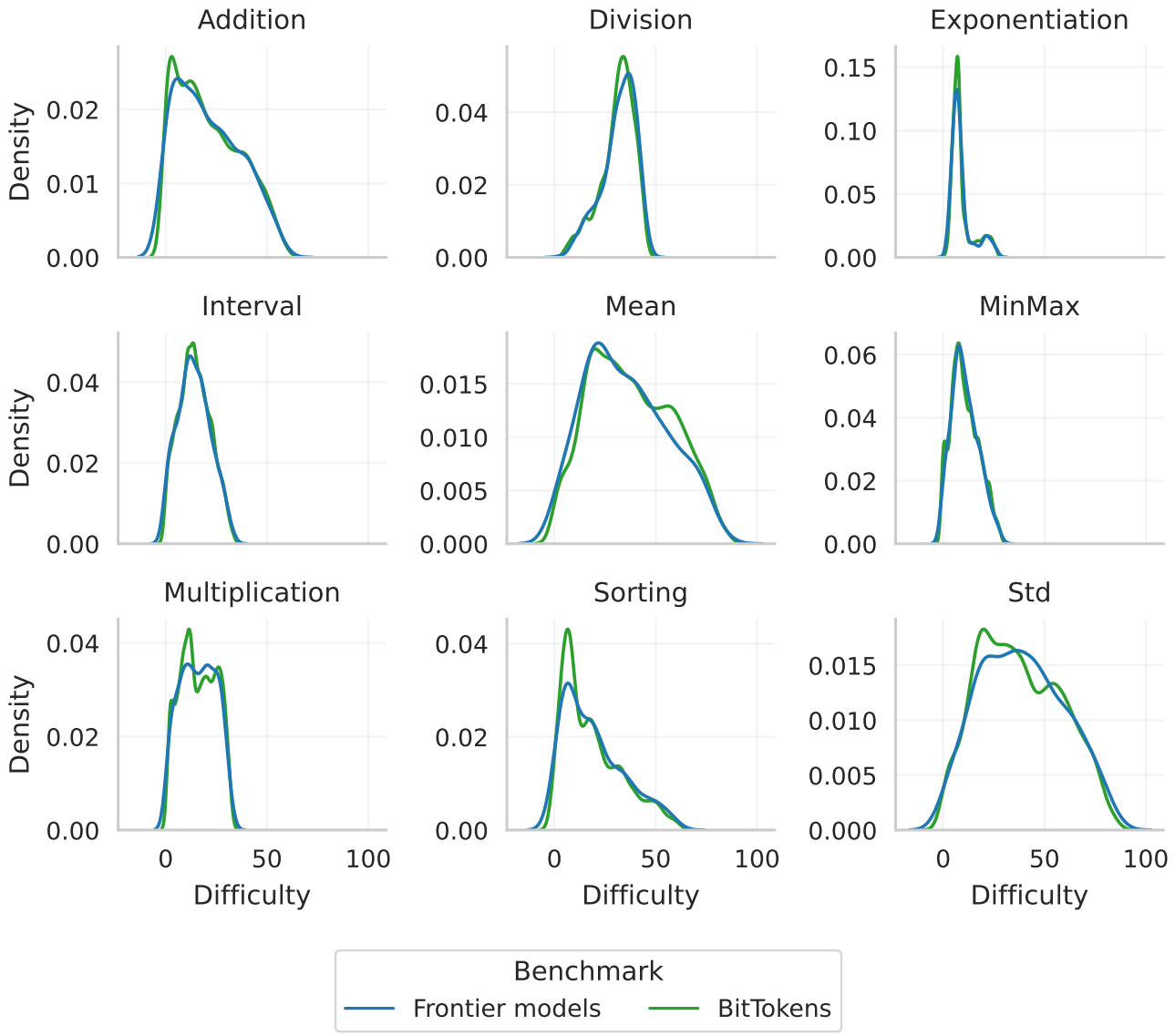

Figure 6. The benchmark for the frontier LLMs is a 500 sample subset of the BitTokens test, but follows the same difficulty distributions.

C. Frontier benchmark results

C.1. Frontier large language models:

We benchmark eight frontier LLMs (DeepSeek-AI, 2024; Comanici et al., 2025; Meta, 2025; Team et al., 2025; OpenAI, 2025; Agarwal et al., 2025; Yang et al., 2025a) – both open and closed source – under maximal and minimal reasoning settings. 'Maximal' reasoning means that we select 'high' reasoning for GPT 5 and GPT OSS 120B, set a thinking budget of 32768 tokens for Gemini 2.5 Pro , and set a budget of 24576 tokens for Gemini 2.5 Flash. All models with permanently enabled reasoning on were also labeled 'Maximal'. 'Minimal' reasoning means that we set reasoning to 'minimal' for GPT 5, and we set a thinking budget of 128 tokens for Gemini 2.5 Pro. Models without reasoning or where it can be completely disabled are denoted as 'None' reasoning models. All models use subword or triple digit tokenization for numbers, except Gemini 2.5 Flash and Gemini 2.5 Pro, which use single digit tokenization.

C.2. log-sMAPE performance

Model	Reasoning	Add	Mult	Div	Mean	Std	MinMax	Interval	Sort	Exp
GPT OSS 120B	maximal	97.6	95.8	80.0	95.6	46.6	99.2	100.0	99.0	56.0
Qwen3 235B 2507	maximal	98.7	88.0	77.8	94.5	48.8	100.0	100.0	99.8	56.9
Qwen3 235B 2507	none	87.5	39.0	46.4	59.4	12.5	95.8	98.6	98.8	21.7
DeepSeek v3.1	maximal	97.0	85.3	84.2	95.0	40.9	99.8	99.8	99.6	48.6
DeepSeek v3.1	none	94.1	38.5	40.8	66.2	15.5	99.8	81.4	99.6	21.0
Kimi K2 0905	none	89.6	44.5	46.8	67.4	13.6	99.6	96.8	98.4	19.9
Llama 4 Maverick	none	79.1	33.3	35.8	60.0	11.8	99.4	76.0	95.6	20.1
GPT 5	maximal	100.0	99.5	96.7	96.1	74.4	100.0	100.0	99.8	78.6
GPT 5	minimal	93.7	30.9	29.5	58.2	16.5	98.8	92.4	98.4	19.0
Gemini 2.5 Pro	maximal	97.4	64.3	74.8	94.3	29.9	100.0	100.0	99.8	45.0
Gemini 2.5 Pro	minimal	99.6	43.4	51.3	81.9	13.0	100.0	99.6	100.0	25.5
Gemini 2.5 Flash	maximal	96.4	44.9	56.3	91.6	27.5	100.0	100.0	100.0	28.9
Gemini 2.5 Flash	none	92.8	32.8	45.2	67.6	13.6	100.0	99.2	99.8	20.3

Table 1. Average performance of each frontier model on each task. The performance of addition (Add), multiplication (Mult), division (Div), exponentiation (Exp), standard deviation (Std), and mean are all measured in log-sMAPE. The performance of MinMax, Interval, and Sorting are all measured in exact match accuracy.

C.3. Exact match accuracy

Model	Reasoning	Add	Mult	Div	Mean	Std	Exp
GPT OSS 120B	maximal	89.4	87.2	45.4	71.2	12.6	13.4
Qwen3 235B 2507	maximal	92.0	64.2	47.0	71.0	12.8	10.4
Qwen3 235B 2507	none	64.4	18.2	15.6	37.2	3.0	3.4
DeepSeek v3.1	maximal	92.4	63.6	54.0	71.2	11.0	10.6
DeepSeek v3.1	none	74.6	20.2	16.4	42.6	3.4	3.2
Kimi K2 0905	none	70.2	23.2	21.0	44.0	2.6	2.8
Llama 4 Maverick	none	50.0	15.6	13.6	34.6	2.2	2.8
GPT 5	maximal	98.4	97.8	91.4	73.8	34.4	46.8
GPT 5	minimal	76.6	14.2	6.6	33.2	3.8	2.4
Gemini 2.5 Pro	maximal	91.0	42.2	48.0	67.6	8.8	8.2
Gemini 2.5 Pro	minimal	82.2	20.6	21.8	55.8	4.4	3.4
Gemini 2.5 Flash	maximal	84.0	27.8	31.6	63.4	7.0	5.6
Gemini 2.5 Flash	none	72.2	13.6	17.4	40.8	2.8	2.2

Table 2. Average performance of each frontier model on each task. The performance metric for addition (Add), multiplication (Mult), division (Div), exponentiation (Exp), mean, and standard deviation (Std) is exact match accuracy on the first 15 significant digits

C.4. Average tokens per problem

Model	Reasoning	Add	Mult	Div	Mean	Std	MinMax	Interval	Sorting	Exp
GPT OSS 120B	maximal	708	1820	3133	446	2056	105	218	193	2815
Qwen3 235B 2507	maximal	3899	5789	8161	3359	8565	965	1379	1248	9889
Qwen3 235B 2507	none	22	22	23	20	23	21	7	63	39
DeepSeek v3.1	maximal	5515	6921	9079	4821	11486	976	1490	1214	9459
DeepSeek v3.1	none	13	12	12	12	13	12	7	34	94
Kimi K2 0905	none	13	78	13	12	45	12	7	33	78
Llama 4 Maverick	none	12	11	12	12	13	12	7	34	13
GPT 5	maximal	3779	8749	16165	3613	19709	585	514	669	28086
GPT 5	minimal	21	21	22	20	21	20	15	39	21
Gemini 2.5 Pro	maximal	4761	11901	11462	4221	9281	574	1013	864	8748
Gemini 2.5 Pro	minimal	108	101	100	111	165	111	173	117	95
Gemini 2.5 Flash	maximal	3084	13698	15390	2494	17751	290	541	382	20149
Gemini 2.5 Flash	none	22	22	22	19	22	20	6	63	22

Table 3. Average number of tokens generated by each frontier model for each problem.

C.5. Performance Stability

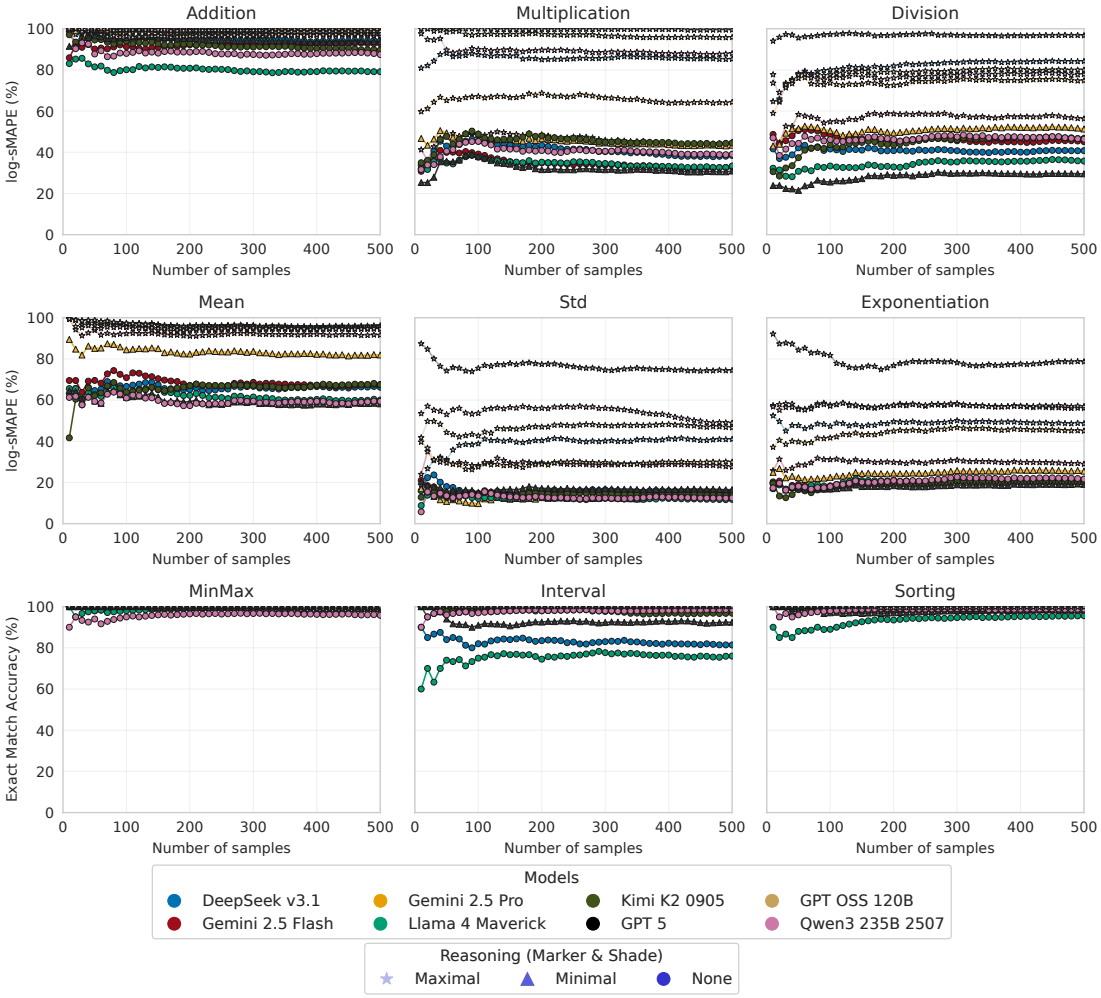

Figure 7. Due to cost constraints we had to subset the full set of 10,000 test samples to 500 samples per task when evaluating the frontier LLMs. We observe performance to already be stable at 500 samples.

D. Experimental setup

D.1. Architecture and hyperparameter configuration

We choose the nanoGPT-2 architecture with 6 layers, 6 attention heads, and an embedding dimension of 768, resulting in a model with 117M parameters. Following Jordan et al. (2024a), we use the Muon optimizer (Jordan et al., 2024b) and modernize the standard architecture of GPT-2 by adding rotary positional embeddings (RoPE) (Su et al., 2024), QK-normalization, and flash attention 2 (Dao, 2024) with sequence packing. The dropout probability is set to 0 to avoid interference with number encodings. Following (Jordan et al., 2024a), all non-scalar parameters in the hidden layers are optimized using the Muon optimizer (Jordan et al., 2024b) with a learning rate of 0.02 and momentum of 0.95. All other parameters are trained with the Adam optimizer (no weight decay) using $\beta_1 = 0.9$ and $\beta_2 = 0.95$. Scalar parameters share the same learning rate of 0.02. The embedding layer weights are untied from the output layer and trained with a learning rate of 0.03. All remaining parameters, including both the language and number heads, use a learning rate of 0.004.

Training is performed with a maximum token budget of 10B tokens, a context length of 1024, and an effective batch size of 192. We employ a cosine learning rate scheduler and allocate 10% of the training tokens for warm-up. Additionally, the Muon optimizer uses 300 momentum warm-up steps. Model performance is evaluated every 32 steps for 2 steps on a small validation set, and the sampling ratio is dynamically adjusted based on current results. After training, we select the checkpoint with the best harmonic mean performance across all tasks.

The training objective is standard next-token prediction, excluding the question tokens from the loss computation. The per-token loss is defined as:

$$\mathcal{L}_{\text{total}} = \text{CrossEntropy}(y_{\text{pred}}, y_{\text{true}}) + 10 \times \mathcal{L}_{\text{num}}(n_{\text{pred}}, n_{\text{true}}),$$

where $\mathcal{L}_{\text{num}}$ is either binary cross-entropy, cross entropy, or mean squared error (MSE), depending on the number encoding strategy. For testing, we generate tokens by selecting the token with the highest probability.

D.2. Number parsing

To parse numerical values from text input to transform them into dedicated number tokens, we use the following regex pattern:

Python regex pattern for signed values (BitToken / xVal)

```
r"[-]?(?:(?:0(?!\.[0-9]))|(?:[0-9]*[.][0-9]+)|(?:[1-9][0-9]*))"
```

Python regex pattern for absolute values (FoNE)

```
r"(?:(?:0(?!\.[0-9]))|(?:[0-9]*[.][0-9]+)|(?:[1-9][0-9]*))"
```

The current regex patterns do not parse numbers written in scientific notation as a single value. That is because the use of scientific notation format may be important to the context of the source text. Future work could investigate the use of dedicated tokens for different number formats, such as scientific notation or integer representation.

D.3. Curriculum learning

We observe that small-scale transformer models benefit significantly from curriculum learning when trained on our numerical tasks. To optimize computational efficiency, we implement an automated curriculum scheduler that selects only those samples $\{s_\tau : \delta(s_\tau) \leq \delta_\tau^{\text{frontier}}\}$ whose difficulty does not exceed the current frontier threshold for a given task. For this purpose, we use the difficulty heuristic $\delta(s, \tau)$ defined in Appendix B.3

The initial frontier difficulty is set to $\delta_\tau^{\text{frontier}} = 0.1 \cdot \delta_\tau^{\text{max}}$, and advances once the model's performance surpasses a predefined threshold, $p(\delta_\tau^{\text{frontier}}, \tau) > \zeta$, where $\zeta = 0.9$. To enhance sample efficiency, we use Equation 16 with $\lambda = 0$ to dynamically compute sampling ratios for each difficulty level based on current performance. This strategy helps mitigate catastrophic forgetting while allocating training tokens to areas of greatest need.

To prevent abrupt shifts in the sample distribution during difficulty transitions, we reserve 20% of the task's token budget for difficulty preview. The corresponding sampling ratios are computed using an exponential decay function:

$$r_{\tau,\delta} = 0.2 \cdot \frac{0.8^{\delta-\delta_\tau^{\text{frontier}}}}{\sum_{\delta>\delta_\tau^{\text{frontier}}} 0.8^{\delta-\delta_\tau^{\text{frontier}}}} \tag{13}$$

To ensure models do not stagnate at lower difficulty levels, we gradually reduce the advancement threshold ζ over time, starting from the lowest difficulties. This encourages progression to more complex tasks if mastery is not achieved promptly. The dynamic advancement threshold for a given task and difficulty, at any training step and learning rate, is defined as:

$$\zeta(\tau, \delta, \text{step}, \text{lr}) = \min\left(\frac{S}{\text{step}}, \frac{L}{\text{lr}^{\text{max}} - \text{lr}}\right) \cdot \zeta_0 \cdot \frac{\delta_\tau}{\delta_\tau^{\text{max}}} \tag{14}$$

Here, S and L denote the training step and learning rate, respectively, at which the threshold for the highest difficulty begins to decrease. We set this point at 50% of the total training duration to ensure the model has adequate exposure to all difficulty levels in the dataset.

D.4. Multitask learning

Our final goal is to train a model that can solve all numeracy tasks simultaneously, which requires simultaneously optimizing nine tasks with varying degrees of difficulty. Training is formulated as a multi-task learning problem, aiming to optimize the model's performance $p(\mathcal{T})$ across all tasks $\tau \in \mathcal{T}$ according to the generalized mean:

$$p(\mathcal{T}) = \left(\frac{1}{|\mathcal{T}|}\sum_{\tau\in\mathcal{T}} (p(\tau) + \epsilon)^\lambda\right)^{\frac{1}{\lambda}} \tag{15}$$

The scaling factor λ controls how strongly low performing tasks influence the overall score. We set $\lambda = -1$ for the harmonic mean. Since the individual losses can have different magnitudes, we normalize all losses to 10 after a warmup period. To account for the varying complexities of the tasks, we define a dynamic sampling ratio $r_\tau \in (0, 1)$ with $\sum_\tau r_\tau = 1$ for each mini-batch. Given the performance $p(\tau) \in [0, 1]$ of each task τ and a given time step, we update the sampling ratio by

$$r_\tau^{\text{new}} = \alpha \cdot r_\tau^{\text{old}} + (1 - \alpha) \cdot \frac{(1 - p(\tau))^{1-\lambda}}{\sum_\tau (1 - p(\tau))^{1-\lambda}}\,, \tag{16}$$

where $\alpha = 0.5$ is a momentum parameter. Intuitively, $\lambda < 0$ leads to more aggressive oversampling of low performing tasks. Table 13 compares the effect of different values of λ. This multi-task sampling strategy aims to achieve a balanced performance across all tasks without the need for expensive hyperparameter tuning for each setting. We note that this approach becomes less important for larger training budgets.

E. BitTokens benchmark

E.1. Multi-task results

	Metric	Subword	Single Digit	xVal	FoNE	BitToken (Ours)
Min/Max	↑ Exact match acc	0.991	0.991	0.001	0.859	**0.999**
Interval	↑ Exact match acc	0.993	0.992	0.324	0.997	**1.000**
Sorting	↑ Exact match acc	0.927	0.955	0.000	0.574	**0.998**
Add	↑ log-sMAPE	0.954	0.974	0.092	0.809	**0.989**
Mult	↑ log-sMAPE	0.450	0.893	0.094	0.300	**0.991**
Div	↑ log-sMAPE	0.522	0.681	0.093	0.275	**0.989**
Fineweb	↓ Perplexity	74.83	64.23	102.57	79.78	**48.78**

Table 4. This table shows the exact multi-task performance values reported in Figure 4.

	Subword	Single Digit	xVal	FoNE	BitToken (Ours)
Min/Max	34.1 + 8.5	60.5 + 16.0	11.1 + 2.0	11.1 + 2.0	11.1 + 2.0
Interval	45.1 + 2.0	27.1 + 2.0	15.9 + 2.0	15.9 + 2.0	15.9 + 2.0
Sorting	34.0 + 23.1	60.0 + 58.0	11.1 + 9.5	11.1 + 9.5	11.1 + 9.5
Add	21.6 + 9.6	32.4 + 16.6	5.9 + 2.4	5.9 + 2.4	5.9 + 2.0
Mult	21.2 + 10.3	32.0 + 17.7	5.9 + 2.4	5.9 + 2.4	5.9 + 2.0
Div	22.8 + 9.6	37.9 + 15.4	5.9 + 2.4	6.1 + 2.4	6.1 + 2.0

Table 5. This table shows the mean number of tokens required (input + output) to solve one sample for each task. A large number of output tokens substantially increases generation time, as each output token requires a separate forward pass.

	Metric	Subword	Single Digit	xVal	FoNE	BitToken (Ours)
Add	↑ Exact match acc	0.926	0.962	0.002	0.767	**0.977**
Mult	↑ Exact match acc	0.290	0.784	0.030	0.164	**0.978**
Div	↑ Exact match acc	0.379	0.514	0.013	0.136	**0.982**

Table 6. Here we report the multi-task exact match accuracy for the single-step calculation tasks.

E.2. Solo-task results

	Metric	Subword	Single Digit	xVal	FoNE	BitToken (Ours)
Min/Max	↑ Exact match acc	0.997	**1.000**	0.002	0.909	0.999
Interval	↑ Exact match acc	0.999	**1.000**	0.328	**1.000**	**1.000**
Sorting	↑ Exact match acc	**0.999**	0.998	0.000	0.718	**0.999**
Add	↑ log-sMAPE	0.999	**1.000**	0.090	0.851	0.998
Mult	↑ log-sMAPE	0.564	0.964	0.096	0.328	**0.985**
Div	↑ log-sMAPE	0.564	0.773	0.094	0.236	**0.995**
Exp	↑ log-sMAPE	0.403	**0.450**	0.047	0.366	0.391
Mean	↑ log-sMAPE	**0.976**	0.965	0.060	0.444	0.534
Std	↑ log-sMAPE	0.365	**0.420**	0.057	0.191	0.354
Fineweb	↓ Perplexity	32.56	30.39	29.65	28.67	**28.33**

Table 7. This table shows the performance of each model trained on a single task with the same 10B token budged.

E.3. Ablations

We tested multiple token combination strategies other than our described "Sum" strategy. "Product" multiplies the [NUM] token with the binary representation. "Concat" sets the [NUM] token to zero in the 64 binary representation dimensions before adding. "Zero pad" removes the [NUM] token and inputs the binary representation directly. "Weighted" passes the binary representation through a linear layer. "Weighted + sum" passes the binary representation through a linear layer and then adds it to the [NUM] token. Across token combination strategies (Table 8), performance is stable with the simple sum and zero pad strategies performing best.

Changing the numeric base (Table 9) substantially degrades performance, particularly for multiplication and division, highlighting the importance of base choice. We found that switching to layer norm, or changing the number head as shown in Table 12, did not meaningfully change performance. Curriculum training (Table 11) yields clear improvements over direct multitask training, especially on arithmetic tasks, confirming its necessity for stable convergence. Finally, appending the reciprocal to the encoding improves performance with a negligible performance overhead (Table 10).

	Metric	Sum	Product	Concat	Zero Pad	Weighted	Weighted + Sum
Min/Max	↑ Exact match acc	0.999	0.996	0.997	**1.000**	0.998	0.999
Interval	↑ Exact match acc	**1.000**	**1.000**	**1.000**	**1.000**	**1.000**	**1.000**
Sorting	↑ Exact match acc	0.990	0.967	0.966	**0.992**	0.983	0.989
Add	↑ log-sMAPE	0.989	0.980	0.977	**0.990**	0.985	0.984
Mult	↑ log-sMAPE	0.991	0.828	0.871	**0.992**	0.988	0.986
Div	↑ log-sMAPE	**0.989**	0.849	0.888	0.981	0.947	0.923
Fineweb	↓ Perplexity	48.78	56.26	55.03	**48.29**	49.04	50.99

Table 8. Ablation: Performance in the multi-task setting with different combination strategies of the [NUM] token and the binary number representation.

	Metric	Base 10	Layer norm
Min/Max	↑ Exact match acc	$0.992^{-0.007}$	$0.997^{-0.003}$
Interval	↑ Exact match acc	$0.997^{-0.003}$	$1.000^{+0.000}$
Sorting	↑ Exact match acc	$0.930^{-0.062}$	$0.976^{-0.016}$
Add	↑ log-sMAPE	$0.937^{-0.053}$	$0.981^{-0.009}$
Mult	↑ log-sMAPE	$0.526^{-0.466}$	$0.988^{-0.004}$
Div	↑ log-sMAPE	$0.437^{-0.544}$	$0.987^{+0.006}$
Fineweb	↓ Perplexity	$76.54^{+28.25}$	$50.10^{+1.81}$
Fineweb text only	↓ Perplexity	$82.99^{+31.08}$	$53.94^{+2.03}$

Table 9. Ablation: Performance in the multi-task setting with different base encoding and normalization. Deltas to baseline shown as red (degradation) and green (improvement).

	Metric	BitTokens w/o reciprocal
Div	↑ log-sMAPE	$0.351^{-0.644}$

Table 10. Ablation: Removing the reciprocal to the encoding vector severely reduces performance on the division task.

	Metric	Subword	Single Digit	xVal	FoNE	BitToken (Ours)
Min/Max	↑ Exact match acc	$0.990^{-0.001}$	$0.990^{-0.001}$	$0.002^{+0.001}$	$0.874^{+0.015}$	$0.991^{-0.008}$
Interval	↑ Exact match acc	$0.990^{-0.003}$	$0.991^{-0.001}$	$0.322^{-0.002}$	$0.997^{0.000}$	$1.000^{0.000}$
Sorting	↑ Exact match acc	$0.927^{0.000}$	$0.949^{-0.006}$	$0.000^{0.000}$	$0.622^{+0.048}$	$0.933^{-0.065}$
Add	↑ log-sMAPE	$0.950^{-0.004}$	$0.967^{-0.007}$	$0.093^{+0.001}$	$0.813^{+0.004}$	$0.948^{-0.041}$
Mult	↑ log-sMAPE	$0.339^{-0.111}$	$0.484^{-0.409}$	$0.094^{0.000}$	$0.285^{-0.015}$	$0.385^{-0.606}$
Div	↑ log-sMAPE	$0.433^{-0.089}$	$0.560^{-0.121}$	$0.093^{0.000}$	$0.300^{+0.025}$	$0.376^{-0.613}$
Fineweb	↓ Perplexity	$76.92^{+2.09}$	$72.89^{+8.66}$	$103.86^{+1.29}$	$75.99^{-3.79}$	$77.26^{+28.48}$

Table 11. Ablation: Performance in the multi-task setting without curriculum training. Deltas to baseline shown as red (degradation), green (improvement), and gray (no change).

	Metric	None	Linear	MLP
Min/Max	↑ Exact match acc	0.999	**1.000**	0.998
Interval	↑ Exact match acc	**1.000**	**1.000**	**1.000**
Sorting	↑ Exact match acc	**0.994**	0.992	0.989
Add	↑ log-sMAPE	0.985	**0.990**	0.989
Mult	↑ log-sMAPE	0.993	0.992	**0.994**
Div	↑ log-sMAPE	0.993	0.981	**0.995**
Fineweb	↓ Perplexity	47.69	48.29	**47.50**

Table 12. Ablation: BitToken performance in the multi-task setting with different number output heads. The encoding is either taking directly from the final hidden layer, transformed by a single linearlayer, or transformed by a 2-layer MLP with ReLU activation.

	Metric	harmonic	geometric	arithmetic
Min/Max	↑ Exact match acc	**1.000**	1.000	**1.000**
Interval	↑ Exact match acc	**1.000**	**1.000**	**1.000**
Sorting	↑ Exact match acc	0.992	0.995	**0.997**
Add	↑ log-sMAPE	**0.991**	0.983	0.710
Mult	↑ log-sMAPE	**0.995**	0.990	0.979
Div	↑ log-sMAPE	0.981	**0.995**	0.978
Fineweb	↓ Perplexity	**48.29**	53.13	77.28

Table 13. Ablation: BitToken performance in the multi-task setting with different task sampling strategies. We compare aggressive oversampling for low performing tasks using the harmonic mean ($\lambda = -1$), moderate oversampling using the geometric mean ($\lambda = 0$), and performance independent sampling using the arithmetic mean ($\lambda = 1$).

	Metric	Single Digit with $r_\tau^{\max}$ =				BitToken with $r_\tau^{\max}$ =			
		0.1	0.2	0.3	1	0.1	0.2	0.3	1
Min/Max	↑ Exact match acc	**0.988**	0.985	**0.988**	**0.988**	**0.999**	0.996	0.989	0.990
Interval	↑ Exact match acc	**0.991**	0.989	0.990	**0.991**	**1.000**	**1.000**	0.999	**1.000**
Sorting	↑ Exact match acc	**0.927**	0.897	0.909	0.911	**0.980**	0.963	0.920	0.922
Add	↑ log-sMAPE	**0.965**	0.954	0.947	0.957	**0.965**	0.944	0.905	0.922
Mult	↑ log-sMAPE	**0.797**	0.654	0.591	0.625	**0.985**	0.971	0.895	0.932
Div	↑ log-sMAPE	**0.550**	0.453	0.430	0.439	**0.983**	0.966	0.896	0.931
Exp	↑ log-sMAPE	0.253	0.292	0.311	**0.313**	0.312	0.355	0.363	**0.374**
Mean	↑ log-sMAPE	0.779	0.789	0.817	**0.819**	0.381	0.485	0.486	**0.489**
Std	↑ log-sMAPE	0.214	0.237	0.357	**0.358**	0.214	0.306	0.304	**0.324**
Fineweb	↓ Perplexity	**72.29**	80.50	88.37	90.37	**55.22**	69.22	81.44	82.26

Table 14. Ablation: Single digit and BitToken performance in the multi-task setting including difficult tasks with capped maximum task ratio $r_\tau^{\max}$. Best values per model are marked in bold.

E.4. Failure mode analysis of the Mean task

As discussed in Section 6, BitTokens struggle to solve multi-step tasks within a single forward pass in our experimental setup. We conducted further analysis to better characterize the limits of the tested model and identify promising directions for further work. Figure 8a compares BitToken performance with the GPT-5 minimal reasoning benchmark model as a function of our difficulty metric. Both models exhibit a similar trend, suggesting that even frontier models struggle with the same class of difficult problems as BitTokens.

To understand the source of this difficulty, we plotted model performance as a function of exponent spread and average exponent in Figure 8b. The resulting heatmap shows that performance deteriorates rapidly once the exponent spread exceeds the average exponent. Intuitively, this transition corresponds to whether the numbers in the input sequence share a long common prefix. For example, consider the following two lists:

Common prefix	**No common prefix**
$[\mathbf{5231}.41, \mathbf{5231}.67, \mathbf{5231}.92]$	$[0.0041, 52.31, 8417.9]$

In the first case, the numbers share the prefix "5231", meaning that only the remaining digits contribute significantly to the computation of the mean. The task therefore reduces to averaging a small residual component. In the second case, the exponents differ substantially, so there is no shared prefix structure that can simplify the computation. The model must instead consider all digits to compute the result accurately.

Figure 9 illustrates the training dynamics of the curriculum for the mean task. The model first learns to compute results for inputs with long common substrings and gradually improves on increasingly difficult samples, up to difficulty level 13. Beyond this point, performance plateaus, suggesting that the model has reached the limit of what it can reliably compute within a single forward pass. As training continues, the curriculum scheduler lowers the advancement threshold, encouraging the model to continue training on more difficult samples.

Although BitTokens appear to be constrained primarily by the model's capacity, the single-digit and subword tokenization schemes perform slightly better on the Std and Exponentiation tasks, and are able to nearly solve the Mean task. We hypothesize that this performance gap arises from differences in available computational steps. Traditional multi-token number tokenization models effectively provide $L \times T$ total layers, where L is the number of layers and T is the number of generated digits, enabling iterative refinement of the numerical output. In contrast, the BitToken head must resolve the entire arithmetic operation within the fixed depth L of a single pass.

In the multi-token setting, previously generated digits can serve as an external scratchpad for storing intermediate state variables such as partial sums or carry information. For instance, the model may first estimate coarse partial sums in the initial forward passes and use subsequent tokens to recursively refine the residual

$$S_{total} - \sum_{k=1}^{T-1} d_k \cdot 10^{-k}. \tag{17}$$

This permits a hierarchical decomposition of the computation that is unavailable to the BitToken model, which must instead compress the full high precision result into latent representation in a single step. Consequently, BitTokens encounter a bottleneck once the complexity of the arithmetic operation exceeds the effective parallel circuit depth of the model.

Future work should investigate whether intermediate auxiliary steps improve performance of BitTokens for complex arithmetic tasks. Once the model's maximum single-forward pass capacity has been defined, larger computations could potentially be decomposed into optimally sized chunks to maximize efficiency.

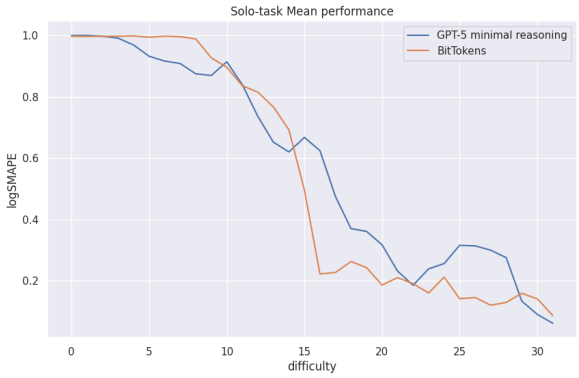

(a) The Mean task performance of BitTokens and GPT-5 with minimal reasoning show a similar performance curve. The chosen difficulty metric directly correlates with the models' performances.

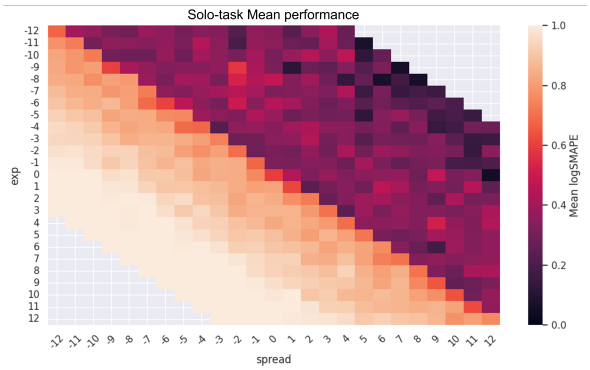

(b) The performance drops sharply once the spread of the list is larger than the magnitude of the list's mean since there exists no common substring anymore.

Figure 8. The performance of BitTokens for the Mean task in the solo task setting, with the difficulty of a sample defined as $\delta_{\text{Mean}} = \text{spread} - \exp + 15$.

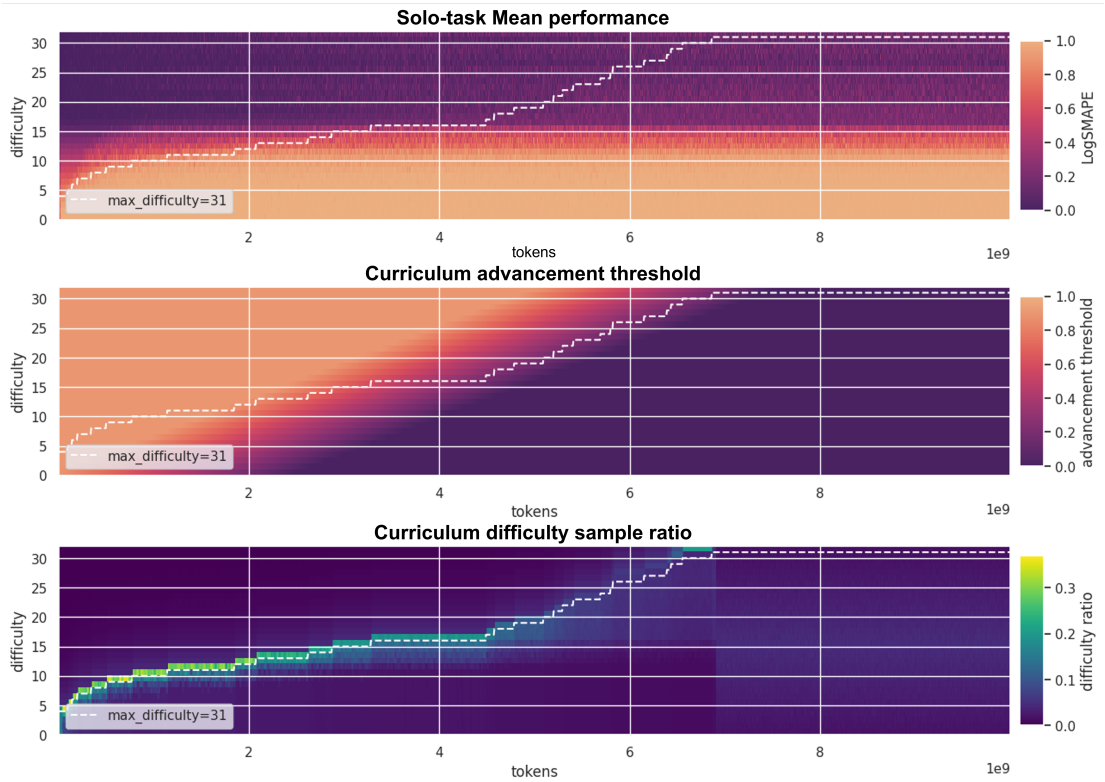

Figure 9. Visualization of the BitTokens curriculum training for the solo-task Mean setting. The difficulty metric does align with the model's performance, but progress plateaus once the model's single forward pass capacity is reached.